International Journal of Engineering Trends and Technology
ISSN: 2231–5381 / https://doi.org/10.14445/22315381/IJETT-V72I4P135
Volume 72 Issue 4, 344-365, April 2024

Original Article

Structural Analysis of an Aircraft Wing with Slotted Flap for Various Materials

Radha Krishnan P[1,2*], Mukesh R[3], Inamul Hasan[1], Srinath R[2,4]

[1]*Department of Aeronautical Engineering, ACS College of Engineering, Karnataka, India.*
[2]*Department of Aeronautical Engineering, Visvesvaraya Technological University, Karnataka, India.*
[3]*Department of Aerospace Engineering, ACS College of Engineering, Karnataka, India.*
[4]*Department of Aerospace Engineering, RV College of Engineering, Karnataka, India.*

[*]*Corresponding Author : krishaeronautics@gmail.com*

Received: 28 October 2023 Revised: 09 March 2024 Accepted: 01 April 2024 Published: 24 April 2024

Abstract - *The wing is the structural component of an aircraft that produces the necessary lift to the aircraft during the flight. When the flow passes over the wing, the pressure difference occurs on the upper and lower surfaces, which is the reason for the lift produced. Flaps affect the aircraft's performance during takeoff and landing. This research aims to analyze the aircraft wing using Al -2024, Carbon fiber (Hexcel AS4C), and graphene at the flap without changing the properties of the wing. Since carbon fiber is a lightweight material and graphene is a self-healing material, they can be substituted for one another in the flaps, and the structural characteristics can be determined to determine which material is best. In this research work the validation is carried out using the previous results; the structural analysis for the reference model was done and compared with the data in the reference paper to validate the research work. The wing with two spars and 5 ribs is modeled in CATIA V5, which is numerically and structurally analyzed using HyperMesh Optistruct. The modeled wing is numerically analyzed to know the pressure force acting on the wing and flaps. This pressure force is given as the load in the static analysis, and the Material properties of the flaps are varied, keeping the material properties of the wing constant. The displacement and strain are less for the Graphene material than the other two materials; hence, the graphene can be used for the flaps than the other two materials.*

Keywords - *Displacement, Flap, Graphene, Natural Frequency, Static Analysis.*

1. Introduction

An aircraft's wing is a vital part that helps it stay in the air. When the aircraft's engine starts, it sucks in air through an opening called the inlet. This air is then compressed in the engine's compressor, making it more pressurized. Afterwards, the air mixes with fuel and gets burned in the engine's combustion chamber. When the hot and high-pressure gases accelerate through the engine's nozzle, they create a force called thrust, which pushes the aircraft forward. As the aircraft moves forward, air flows over its wing, which is designed to be streamlined because of the wing's streamlined shape and a principle called Bernoulli's principle. In this, the fluid particle moves faster over the top surface of the wing and slower in the lower surface of the wing. This difference in pressure distribution generates lift, which helps keep the aircraft in the air. Wings need to be strong relative to their weight and capable of enduring repeated stresses during flight. High-lift devices on wings, like slats and flaps, significantly affect the aircraft's performance during takeoff and landing. They can improve payload capacity and fuel efficiency and reduce noise around airports. Efficient high-lift devices that simplify the wing's structure can also reduce weight, production costs, and maintenance expenses. Slats and flaps are examples of high-lift devices. They are designed to increase the amount of lift a wing can produce. They work by changing the wing's shape and effectively making it larger.

The aviation industry is growing fast, and to keep up, there are improvements in the materials used in aircraft. The main reasons for these improvements are to reduce costs, make aircraft lighter, and make the parts last longer. Using lightweight materials helps planes work better, using less fuel, flying farther, and carrying more weight, all of which lower the cost of running an aircraft. Scientists are working to develop materials that are strong, lightweight, resistant to corrosion, and better able to handle damage. Selecting the right material is super important when designing an aircraft. Nowadays, a lot of military and commercial planes, as well as drones, use composite materials a lot. In the past, aluminium-based alloys were mostly used in aviation. These alloys are good because they are heavy, resist corrosion, can handle damage, and work well at high temperatures, which is important for high-performance aircraft. But now, materials like fiber-reinforced composites made of things like SiC-SiC and C-SiC are taking the place of old materials in important aircraft parts. These new materials are helping make lightweight structures, which is a big deal in aviation.

A number of special requirements related to the structural elements should be considered during the manufacturing of aircraft wings. The two main functional requirements to be taken into account when choosing materials for the construction of aircraft wings are high strength and lightweight. In the past, airplanes were primarily made from metal alloys like aluminum. Nowadays, materials like silicon carbide metal matrix composites have altered conventional metals. These composites are lighter and offer advantages like reduced maintenance, high resistance to wear and tear, and increased fuel efficiency. They provide a higher strength-to-weight ratio and stiffness-to-weight ratio compared to metals.

Computational Fluid Dynamics (CFD) is a crucial tool for studying how fluids behave in various situations, including those involving heat and mass transfer. It works by using computer simulations to solve complex equations that describe fluid movement, called the Navier-Stokes equations, which are difficult to solve by hand. CFD helps engineers get very close approximations of how fluids flow in different scenarios. One important application of CFD is in designing advanced high-lift devices.

These are components used in aircraft to increase lift during takeoff and landing. High-lift devices, like flaps, change the shape of the wing to generate more lift without increasing the angle at which the aircraft is tilted. This is important because it allows planes to take off and land safely at lower speeds. CFD is helping engineers predict how these high-lift devices affect the aerodynamics of an aircraft. They need to know things like the maximum lift the aircraft can generate and the balance between lift and drag. This helps in designing more efficient and safer aircraft. One challenge in studying high-lift systems is that they create complex flow patterns with issues like airflow separation and turbulence.

Engineers use CFD, along with experiments, to better understand and improve these systems. For example, flaps on the wings increase lift by changing the wing's shape. They make the wing more curved, which increases the maximum lift it can generate. However, this also reduces the angle at which the wing can operate before stalling (losing lift). To counter this, large commercial aircraft use slats, which are like small wings at the front of the main wing. This helps maintain lift even at higher angles, making landings safer. The presence of flaps also affects the airflow over the main wing. It creates a swirling motion (vortex) near the wing's back edge, which increases lift. So, engineers use CFD to understand how these flaps and the air around them work together to make planes safer and more efficient during takeoff and landing. In the last twenty years, modal analysis has become an important tool for understanding and improving how things move and vibrate in engineering. It is not just used in mechanical and aeronautical engineering; it is also applied in civil engineering, biomechanics, space technology, acoustics, transportation, and nuclear plants. Modal analysis helps us understand how things naturally vibrate or oscillate when they are not being pushed or pulled by outside forces.

When something vibrates freely, it does so at specific frequencies that depend on its properties, like how stiff it is and how its mass is distributed. For really complex systems, like structures made up of many parts, we use modal analysis to figure out how they move and vibrate. This is super useful in various fields, from identifying and understanding vibrations to checking the integrity of structures, making improvements, and detecting damage. In engineering, when designing things, we need to calculate stuff like how much something will move, how it will handle stress, its natural vibration frequencies, and how it will deform. We use mathematical models that consider things like mass, stiffness, and shape. However, sometimes, these values are not exact due to variations in materials or how things are put together during manufacturing.

Self-healing materials are materials that can heal on their own when damage occurs and gain their original properties that are intrinsically such that the lifespan can be extended. Graphene is a material which is a single-layer carbon structure that contains outstanding heat, mechanical, and electrical properties.

Self-healing materials, which are made using graphene based, are huge impactful materials in practical application, and their application is very extensive; they are used in military equipment, aircraft, automobiles, electronic components and building materials. Carbon fibers are less-weight materials with several advantages, like high tensile strength with a high strength-to-stress ratio, high resistance to chemical reactions, high stiffness, and less thermal expansion. They had a huge application in aerospace, military, and civil engineering due to their properties. Aircraft Industries always tries to reduce the operating cost of aircraft by introducing innovative techniques [4,20]. So, this paper concentrates on that point by introducing lightweight and smart materials which have the self-healing effect. Lightweight materials reduce fuel consumption, and Smart materials, which have a self-healing effect, reduce the frequency of maintenance work, which in turn reduces the operating cost of the aircraft. So, in this research, Carbon fiber (Hexcel AS4C) and graphene are taken for the lightweight and smart materials and results are compared with the conventional aluminum Al 2024 material. Graphene material shows better results compared with other materials.

2. Literature Review

Guanghao et al. (2019) summarized the properties of the self-healing materials, which are made using graphene in the self-healing methods, synthesis method and specific applications. They concluded that the introduction of graphene partially removed the restriction on self-healing properties. Mekalke et al. (2016) determined the mode shapes and natural frequency of different materials for cantilever beams. The researcher also studied the shear effect and spring-mass systems on the dynamic behavior of the beams experimentally and numerically using the software. They formulated the equation of motion for the cantilever beam to find out the natural frequency analytically by using the Euler-Bernoulli equation. They used ANSYS 12.0 software to find the natural frequency numerically for 15 beams for three different materials. They used materials like Mild steel, Aluminum and Glass fiber. They concluded that the error between software and analytical is low at lower frequencies; it increases with the increase of frequencies, and they found that the natural frequency is Aluminum and Mild Steel is lesser than the Glass Fiber.

Salu et al. (2018) modeled a wing of a trainer aircraft with 15 ribs and 2 spars using CATIA V5 R20 software. The researchers had done static structural analysis for finding the stress, strain and induced deformation and modal analysis for finding the frequency and vibration using ANSYS software for the Carbon fiber reinforced polymer, Glass fiber reinforced polymer and Aluminum 2024 T3 and compared their results. They found that Epoxy carbon has low weight, minimum deformation, and better strength than the Al 2024T3. Rajappan et al. (2013) conducted experiments using a wing made of single-piece laminated composite materials. They applied different types of forces, such as the wing's own weight and the force of gravity, in different directions: along the wing, across the wing, and vertically. They compared the stress and deformation of the wing under these various loads. They discovered that when multiple types of forces were applied together, the stress and deflection values differed from when each force was applied individually. Sivarama et al. modeled a wing of a trainer aircraft with 15 ribs and 2 spars using PRO-Engineer WILDFIRE 5.0 software. The researchers had done static structural analysis for finding the stress, strain, deformation and factor of safety and modal analysis for finding the frequency and using finite element approach with the help of ANSYS software for carbon epoxy, S2 glass and Al 6061-T8 and compared their results. They observed in structural analysis that the stress value increases with the increase of wing speed; Carbon epoxy has less stress value and more strength than the other two materials. In modal analysis, that deformation and frequency are higher in carbon epoxy.

Performed analysis for the wing for AMTAS and the new design at a constant temperature using ANSYS 14.0 software and compared their results. In the new design, they changed the twist angle by ± 10% at the fixed and free end of the wing and used AISI6061-T6 material for both designs. They found that the factor of safety has increased by 43% for the new design at the fixed end. Vinay et al. (2021) modeled a wing of trainer aircraft using NACA 64215 airfoil with 15 ribs and 2 spars and winglets with cant angles of 25° and 45° using CATIA V5 R20 software. The researchers had done static structural analysis to find the stress, strain and induced deformation using ANSYS software for the S2 glass, Kevlar-49 and Boron fiber materials and compared their results. They concluded that the wing with a winglet of 45° cant angle and boron fiber materials is the better model than the other since it has less stress value. Pugazhenthi et al. (2018) modeled a tapered wing without ribs and spars having carbon epoxy and aluminum alloys as material and NACA 4412 as an airfoil. They applied the self-load due to the gravity in various material axes in ANSYS APDL and solved for deformation and stress. They concluded that wing deformation and stress values were changing more in combined load conditions.

Saravanan et al. (2018) numerically investigated the maximum stress concentration at the splice joint of the aircraft wing and fatigue life using NASTRAN and PASTRAN. They concluded that stress is distributed uniformly, but the maximum stress of 182.26 Mpa is obtained at the rivet hole section in the splice joint, and the fatigue failure occurs at 200 Mpa. Kenneth et al. (2017) presented the data from Taguchi's L9 array on low speed and twin wing design and varied the design parameters like altitude, speed, height and stagger. They concluded that the use of twin wings has aerodynamic disadvantages even though negative stagger is in operation, stagger, and separation distance of wings had more influence than the altitude and speed in the aerodynamic performance and separation and stagger are more critical parameters. Christopher et al. (2002) conducted a survey on the CFD methods for the computation of high-lift multi-element configurations involving 2D and 3D configurations.

They concluded that the pressure due to surface, friction due to skin, drag and lift can be predicted with reasonable accuracy for 2D and 3D flows, and the velocity profile with slat wakes for 2D has the same effect as experiments. David et al. (2016) developed a methodology for integrating the preliminary design of the wing with the trailing edge for the flap mechanism. They compared the study with four different mechanisms used in the Boeing 777 wing. They concluded that there is an underestimation of 13% in weight due to modeling specification in the presented mechanisms. The presented method gave insight into the gap and overlapped behavior of the flap during deployment for the designers. Arnav et al. (2020) compared the aerodynamic coefficients at constant velocity for NACA 2412, 2414 and 2415 airfoils using the standard k epsilon viscosity model in ANSYS software. They found that while different airfoils could be used for various applications, the NACA 2412 airfoil was the best choice for the same application because it has better aerodynamic properties than the other two. Sravan et al. (2018) performed numerical and structural analysis for the wing to obtain a suitable wing design for long-range and endurance for small-scale UAV using Clark Y, Seing-Donovan 7032, and SA 7035 airfoils in ANSYS software at a velocity of 20 m/s.They found that the SA 7035 airfoil is suitable for the requirements and pressure rapidly increases with the increase of angle of attack, and at a 16-degree angle of attack, the drag is more than the lift produced. Ajeet et al. (2020) performed an experimental analysis with thermoplastic polyurethane (TPU) and ethylene vinyl acetate (EVA) foam material. They used additive manufacturing techniques to support less shell-shaped lattice structures and compared the results for both materials.

Yupeng et al. (2022) reviewed room-temperature polyurethanes based on covalent, non-covalent, and dynamic bonds. They summarized the applications of polyurethanes in various fields like leather coatings, flexible materials, biomaterials, etc. Rajendran et al. [2020] have done the experimental analysis of morphing airfoil structures in wings using additive manufacturing and compared the deflection values with computational results. They have used a combination of materials, such as PLA and TPU in the wing prototype. To get the proper shape, stiffness can be added to the materials. John et al. (2016) have reviewed the types, synthesis and uses of polyurethane material which have attractive physical, chemical, and mechanical properties.

It has a wide range of applications in the automobile industry, building and construction field, marine field, medical field, etc.. Also, it has the advantage of recycling and recoverable property. So, it can be chosen over other conventional polymers. Bartlomiej et al. (2021) used hybrid polyurethane coating, which is mixed with Nano silica in NACA 0012 airfoil to reduce ice accretion. Under different Icing conditions, the experimental analysis was carried out in a wind tunnel. Results show that hybrid polyurethane reduced Ice accretion by 65%.

3. Materials and Methods

A literature survey is carried out to know about the previous findings on Self-healing materials, and structural and numerical analysis. From the literature survey, a validation case is identified to validate the present research work. The model in the reference paper is modeled and analyzed statically, and taken the results. These results are compared with the data in the reference paper. The wing is designed with a flap by fixing the airfoil and chord of the wing and flap.

The CFD analysis was carried out in the ANSYS software package. The pressure acting on the upper and lower surface is taken from the post-processing data. This data is given as input in the structural analysis as a load. Then, the material was varied for the flap, and the results were taken for different materials, and the results were compared; the flow of the project is represented in Figure 1.

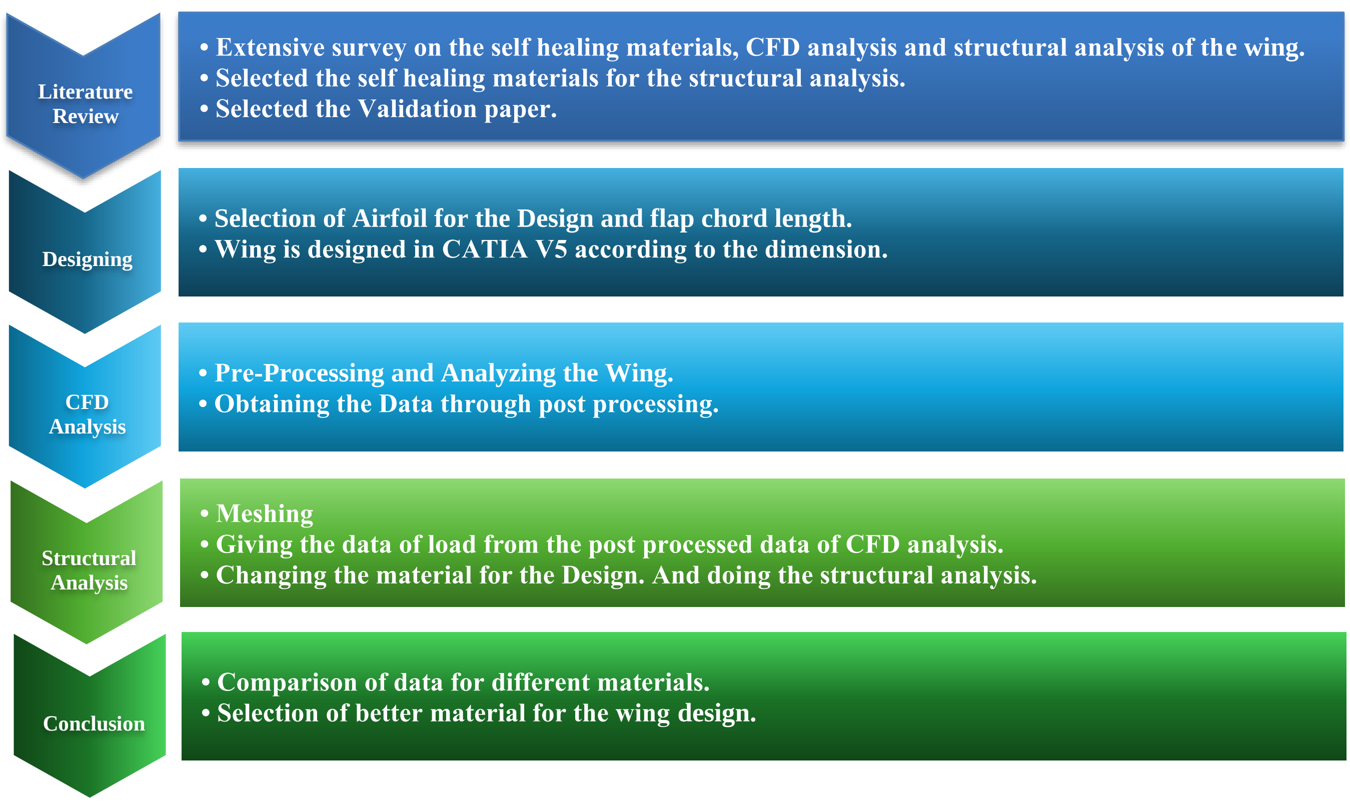

Fig. 1 Methodology

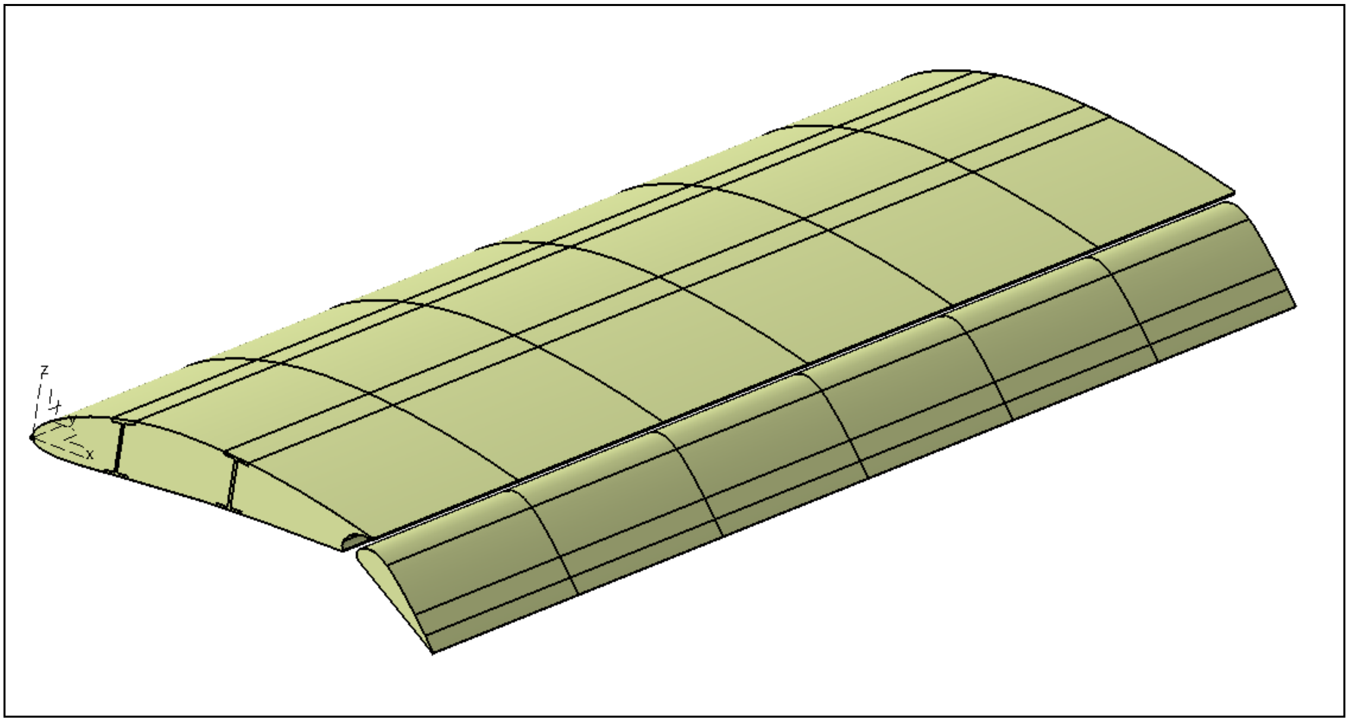

Fig. 2 Wing model

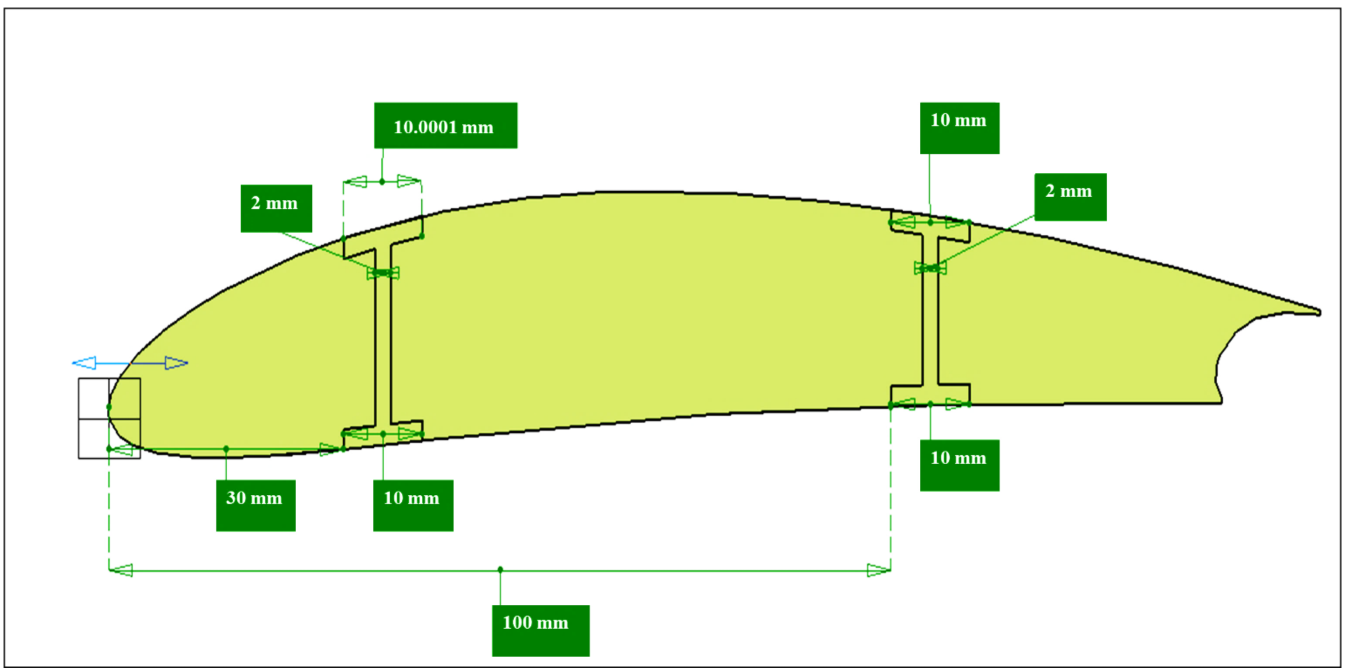

Fig. 3 Front view of the wing

3.1. Design of Wing Model

We studied the effect of fluid flow on a rectangular wing as per the NACA standards, from which the NACA 6412 airfoil is selected for the design of the wing. The wing was modeled in CATIA V5 with a span of 595mm, a chord of 190mm, and a flap chord of 47.5mm, which is 25 % of the wing chord.

The wing consists of two I-section spars and five ribs, which are equally placed. The flaps are deflected to 0°,10°, 20° and 30°. The modeled wing is shown in Figure 2, and the front view is shown in Figure 3.

3.2. CFD Analysis

In the CFD analysis, the mesh is generated using ICEM-

CFD. The generated mesh is transferred into polyhedral cells by not changing the prism cells to improve the quality and convergence in Fluent. The CFD analysis is carried out for the plain wing and four flap deflections at Mach 0.4. In the CFD solver, a Fluent solver is used for the analysis. The boundary conditions taken in fluent software are shown in Figure 4. As per the previous study of this work CFD analysis was done for plain wing and four flap deflections and the results were taken. The pressure contour for 10° flap deflection is shown in Figure 5. The pressure values are taken for the wing and flap spanwise, and the values are listed in Table 1.

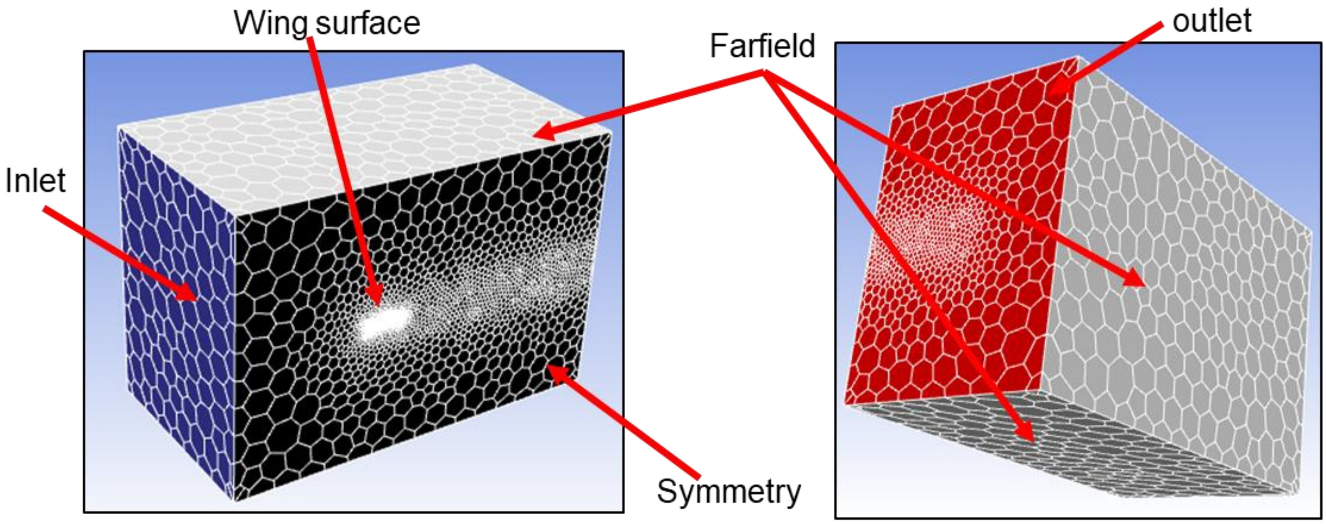

Fig. 4 Boundary conditions

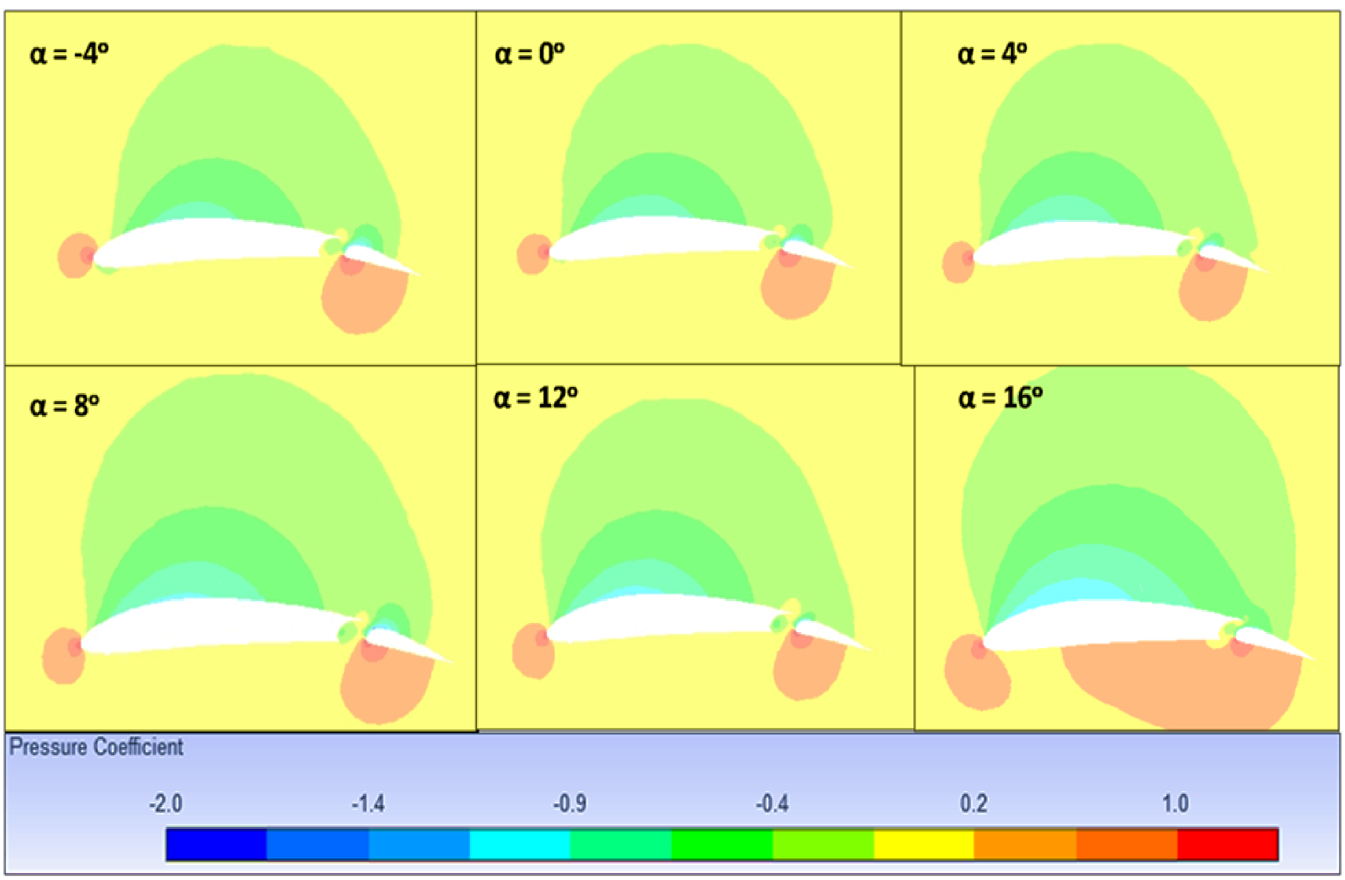

Fig. 5 Pressure contour for 10° flap deflection

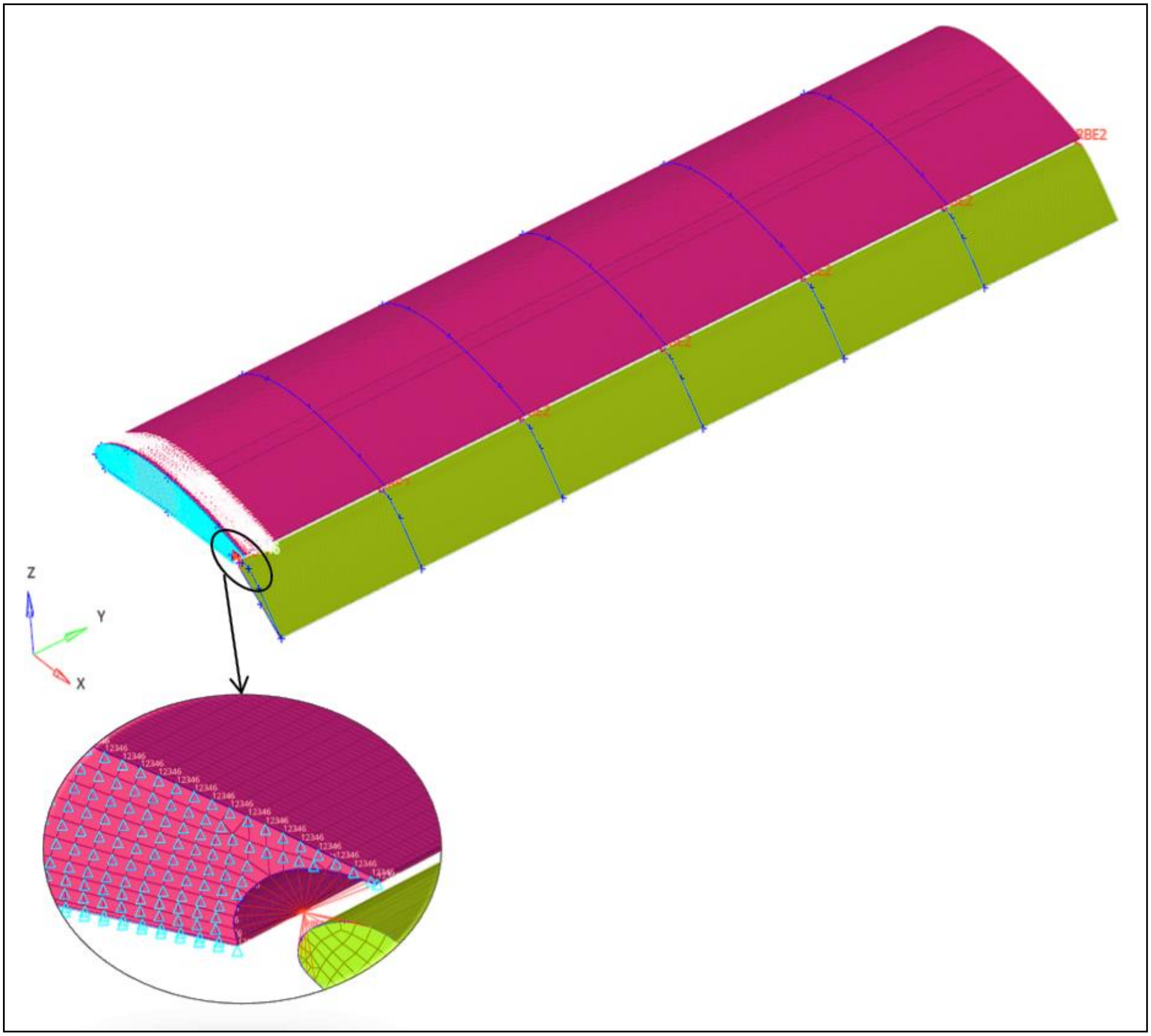

Fig. 6 Constraints on the wing

Table 1. Pressure valued from the CFD Analysis

Y location (mm)	Wing Surface		Flap Surface	
	Lower Surface (N/mm^2)	Upper Surface (N/mm^2)	Lower Surface (N/mm^2)	Upper Surface (N/mm^2)
0	8.209949	2.004482	5.354241	1.226917
10	8.161689	1.991839	5.345409	1.148253
20	8.12143	1.985095	5.344578	1.075489
30	8.07517	1.970401	5.337746	0.994775
40	8.03691	1.953707	5.338914	0.912061
50	7.99265	1.938614	5.334083	0.830948
60	7.95439	1.92252	5.335251	0.748834
70	7.91313	1.907026	5.33342	0.66732
80	7.86487	1.897632	5.324588	0.591906
90	7.826611	1.875839	5.325757	0.504092

100	7.787351	1.867545	5.325925	0.429778
110	7.773495	1.869661	5.320729	0.474611
120	7.76064	1.864777	5.316532	0.512444
130	7.750785	1.862893	5.315336	0.553276
140	7.73793	1.868009	5.31114	0.601109
150	7.726074	1.866925	5.307944	0.642742
160	7.713219	1.869341	5.303747	0.687875
170	7.710364	1.868857	5.309551	0.730108
180	7.697509	1.864673	5.305355	0.76864
190	7.685653	1.862589	5.302158	0.809273
200	7.678798	1.863705	5.303962	0.853106
210	7.652349	1.878143	5.309637	0.739382
220	7.628499	1.892582	5.317913	0.625658
230	7.60495	1.907021	5.326488	0.511935
240	7.588001	1.920459	5.341663	0.397211
250	7.567551	1.935898	5.353338	0.284487
260	7.542102	1.949336	5.360013	0.169763
270	7.518153	1.963775	5.368188	0.056039
280	7.494203	1.978214	5.376364	0.057685
290	7.476654	1.983652	5.390939	0.180408
300	7.459304	2.001691	5.405714	0.290532
310	7.424875	1.987375	5.40247	0.170528
320	7.399446	1.96666	5.408225	0.056924
330	7.374017	1.945944	5.413981	0.05668
340	7.347587	1.923729	5.418737	0.168784
350	7.323158	1.906513	5.425492	0.285888
360	7.296729	1.892798	5.430248	0.406492
370	7.2713	1.872482	5.436004	0.520496
380	7.245871	1.851867	5.441759	0.6342
390	7.220441	1.828651	5.447515	0.745304
400	7.195012	1.813936	5.453271	0.864908
410	7.122028	1.778472	5.551675	0.74655
420	7.046944	1.742008	5.647979	0.627193
430	6.97556	1.715544	5.747984	0.517836
440	6.907076	1.679081	5.850888	0.398479
450	6.835092	1.643617	5.950292	0.280122
460	6.769309	1.607153	6.055897	0.160764
470	6.696525	1.573689	6.154501	0.044407
480	6.620741	1.537225	6.250105	0.07495
490	6.551957	1.499762	6.35271	0.195307
500	6.487173	1.468298	6.459314	0.309664
510	6.551288	1.293253	6.610644	0.381167
520	6.627802	1.108208	6.774375	0.462669
530	6.698217	0.930164	6.932005	0.537172
540	6.768032	0.755119	7.089035	0.608674
550	6.838847	0.574074	7.247066	0.686177
560	6.908061	0.39903	7.403496	0.75768
570	6.979276	0.215985	7.561926	0.837182
580	7.058441	0.03894	7.728307	0.910685
590	7.131705	0.146104	7.888787	0.992187

Table 2. Comparison of hyper mesh results and ansys results

Mode	Mild Steel			Aluminum			Glass Fiber		
	Natural Frequency Results from Hyper Mesh	Natural Frequency Results from Ansys	Error %	Natural Frequency Results from Hyper Mesh	Natural Frequency Results from Ansys	Error %	Natural Frequency Results from Hyper Mesh	Natural Frequency Results from Ansys	Error %
1	11.602	11.423	1.56	11.34	11.604	2.27	11.967	11.968	0.008
2	72.691	71.586	1.54	71.047	72.717	2.29	74.974	75.001	0.03
3	203.481	200.46	1.50	198.879	203.63	2.33	209.871	210.02	0.07
4	398.623	393.02	1.42	389.61	399.23	2.40	411.144	411.77	0.15
5	658.76	650.55	1.26	643.866	660.23	2.47	679.452	681.59	0.31
6	983.786	974.3	0.97	961.543	989.69	2.84			
7	1373.644	1366.5	0.52	1342.586	1388.1	3.27			
8	1828.273	1829.9	0.08	1988.793	1858.9	6.98			
9	2034.801	2123.7	4.18	2106.294	2157.3	2.36			
10	2347.609	2364.9	0.73	2865.302	2402.3	19.27			

Table 3. Properties of the material

Material Properties	Al-2024	Carbon fiber (Hexcel AS4C)	Graphene
Elastic Modulus (Mpa)	73000	231000	680000
Density (Kg / mm^3)	2.7 E-06	1.78 E-06	2.27 E-06
Poisson’s Ratio	0.33	0.3	0.17

3.3. FEA Modal and Structural Analysis

Analysis was performed in this research work by using the finite element method for a wing. Both modal and static analysis were performed using HyperMesh Optistruct. 2D quad and Tria elements are used for the wing, flaps, and ribs and 3D Hexa elements are used in spars. Wing and flap skin sections are connected using RBE2 for the load transfer. Pressure is applied uniformly on the surface using elements varying for each 10mm; here, elements mean the total pressure divided by the total elements on the surface. Three materials were varied for the Structural Analysis, and the materials were Aluminum, Carbon fiber (Hexcel AS4C), and graphene.

The material properties are varied only in the Flaps. Graphene and Carbon fiber (Hexcel AS4C) are self-healing and lightweight materials, they can be substituted for one another in the flaps, and the best material can be chosen by performing static and modal analysis. This pressure value is taken from the CFD results, which are shown in Table 1. Modal analysis is carried out for fix-free conditions, and linear static analysis is carried out for variable pressure distribution on the wing. The front surface of the wing is constrained, as shown in Figure 6. The material properties of the material used in this research work are given in Table 3.

4. Validation of Numerical Analysis

From the literature survey, a validation case is identified. The author in the validation case has found out the natural frequency of the cantilever beams for three different materials, like Aluminum, Mild steel, and Glass fiber, analytically and numerically.

The natural frequency of the cantilever beam made up of Aluminum, Mild Steel, and Glass fiber is found by using Hyper Mesh Opti struct, and the results were compared with the results from the validation case and hence validated. The same procedure with similar boundary conditions is followed in the present research work with Hyper mesh software. Since the Numerical method is validated with the reference paper 10 results, the experimental analysis has not been performed separately here. The Comparison of materials of different materials is shown in Table 2.

The natural frequency obtained from the Hyper Mesh results are compared with the data from reference paper 10 for different materials, which is shown in Table 2. Since Glass fiber natural frequency modes were given only up to 5, validation analysis was also taken up to mode 5—the other materials like mild steel and aluminum, natural frequencies taken till Mode 10. Based on the error percentage comparison, it can be concluded that the boundary conditions were acceptable for the numerical analysis.

5. Results and Discussion

The results of the modal and static analyses are discussed in this section. Figures 7 to 9 show the results of the modal analysis of the Al-2024 material's wing and flap, as well as the flap made of Carbon fiber (Hexcel AS4C) and graphene material, while maintaining the wing with constant material.

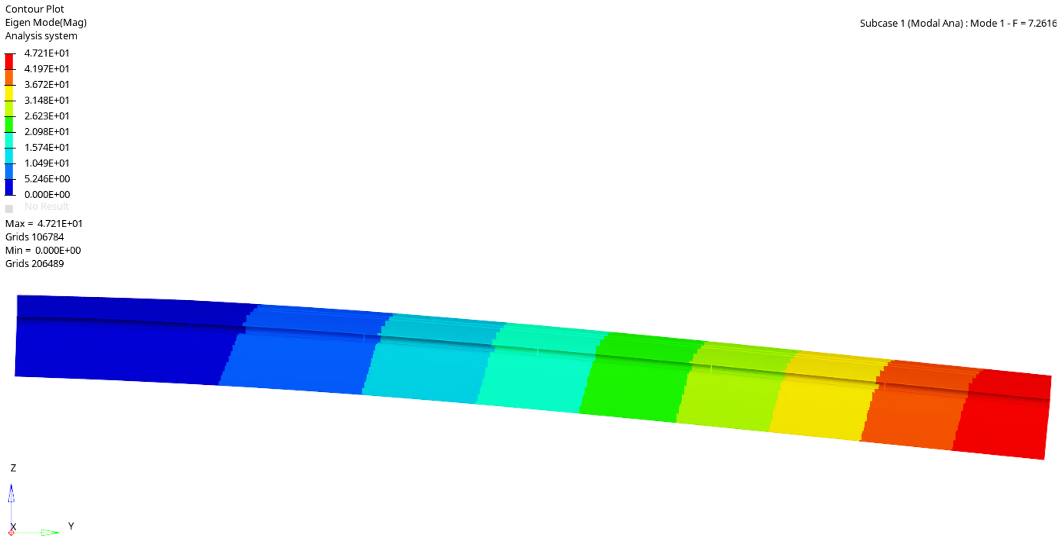
Contour Plot
Eigen Mode(Mag)
Analysis system
4.721E+01
4.197E+01
3.672E+01
3.148E+01
2.623E+01
2.098E+01
1.574E+01
1.049E+01
5.246E+00
0.000E+00
No Result
Max = 4.721E+01
Grids 106784
Min = 0.000E+00
Grids 206489
Subcase 1 (Modal Ana) : Mode 1 - F = 7.2616
Z
X
Y

(a)

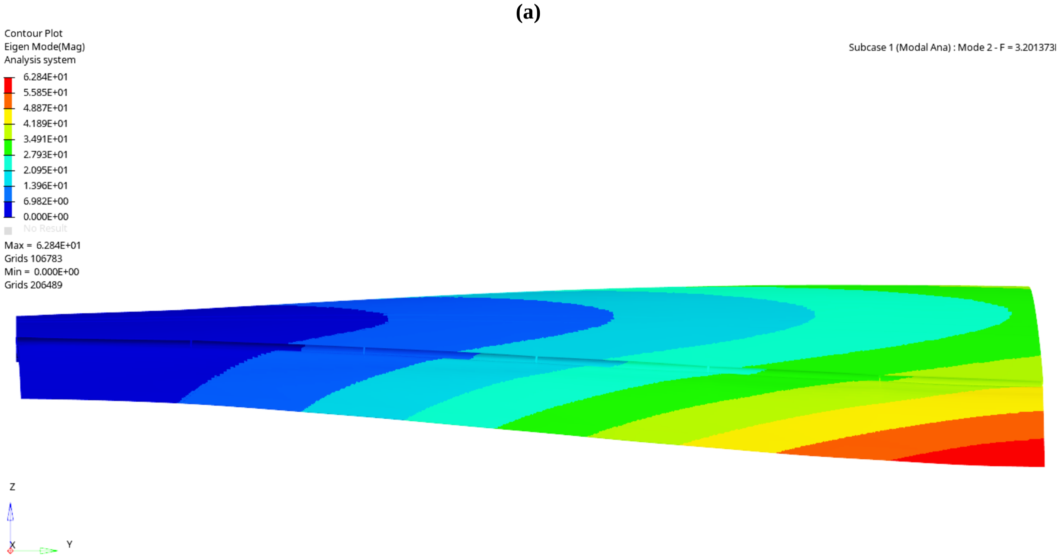
Contour Plot
Eigen Mode(Mag)
Analysis system
6.284E+01
5.585E+01
4.887E+01
4.189E+01
3.491E+01
2.793E+01
2.095E+01
1.396E+01
6.982E+00
0.000E+00
No Result
Max = 6.284E+01
Grids 106783
Min = 0.000E+00
Grids 206489
Subcase 1 (Modal Ana) : Mode 2 - F = 3.201373
Z
X
Y

(b)

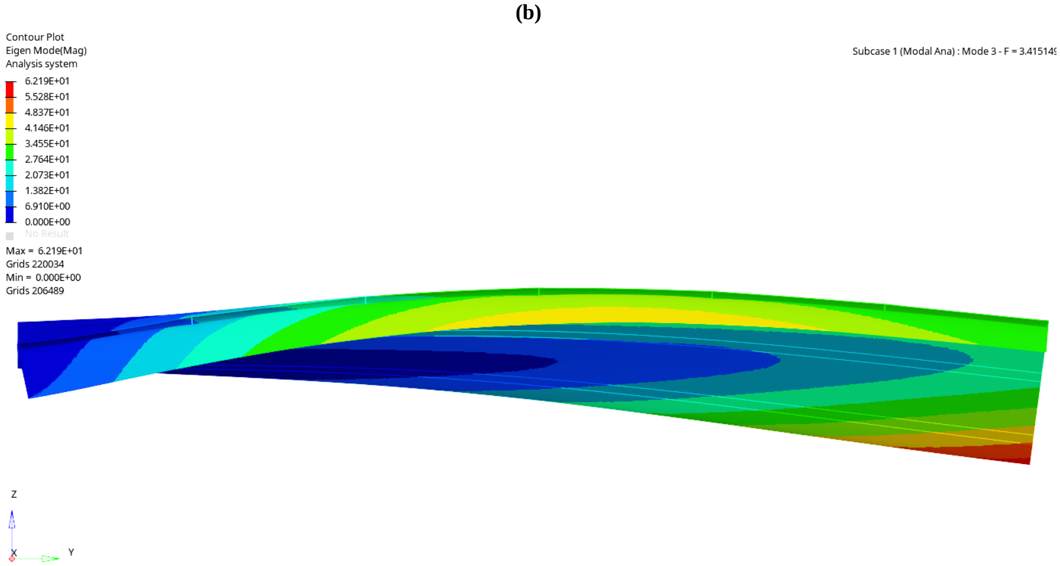
Contour Plot
Eigen Mode(Mag)
Analysis system
6.219E+01
5.528E+01
4.837E+01
4.146E+01
3.455E+01
2.764E+01
2.073E+01
1.382E+01
6.910E+00
0.000E+00
No Result
Max = 6.219E+01
Grids 220034
Min = 0.000E+00
Grids 206489
Subcase 1 (Modal Ana) : Mode 3 - F = 3.41514
Z
X
Y

(c)

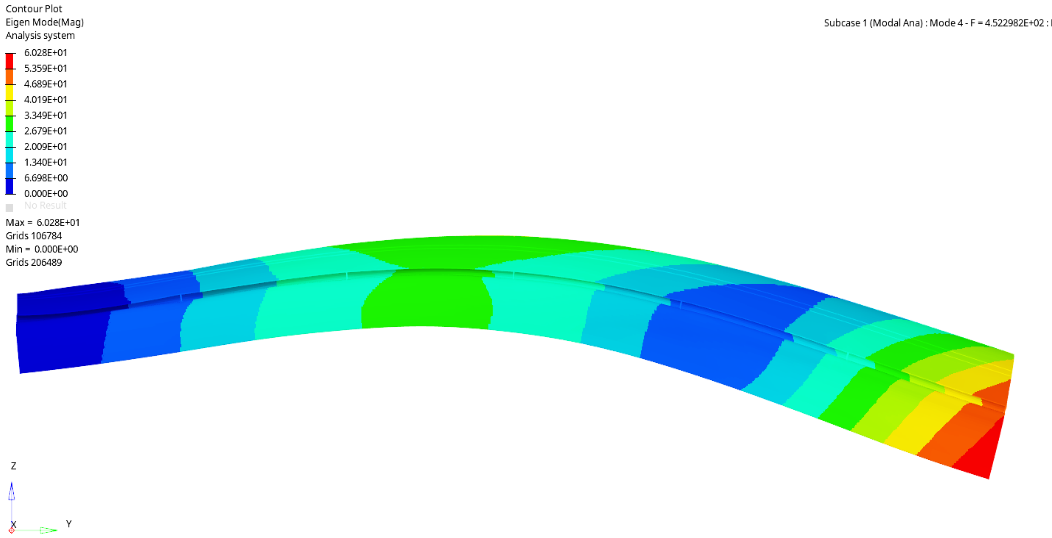

(d)

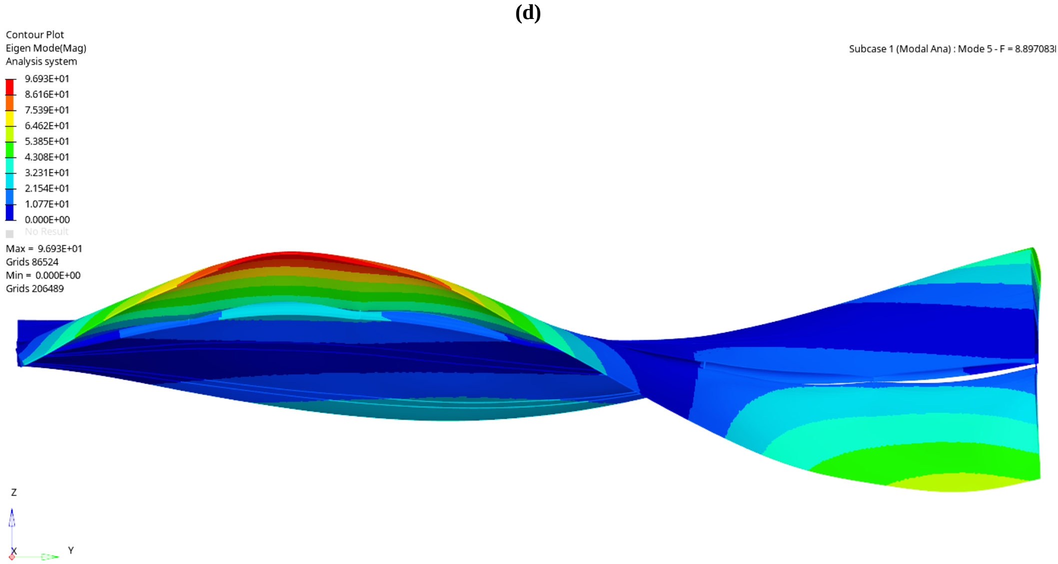

(e)

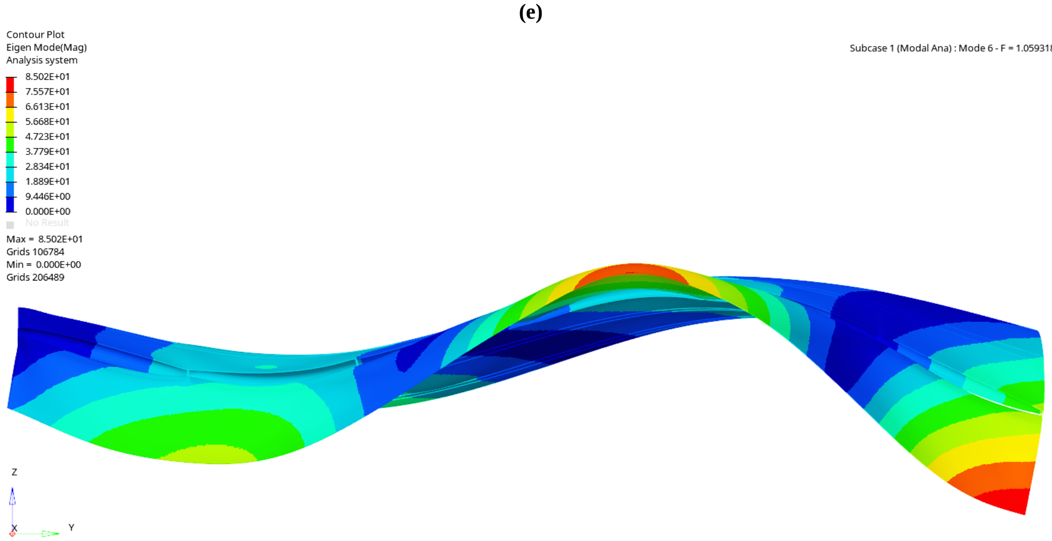

(f)

Fig. 7 Modal analysis of Al-2024 material

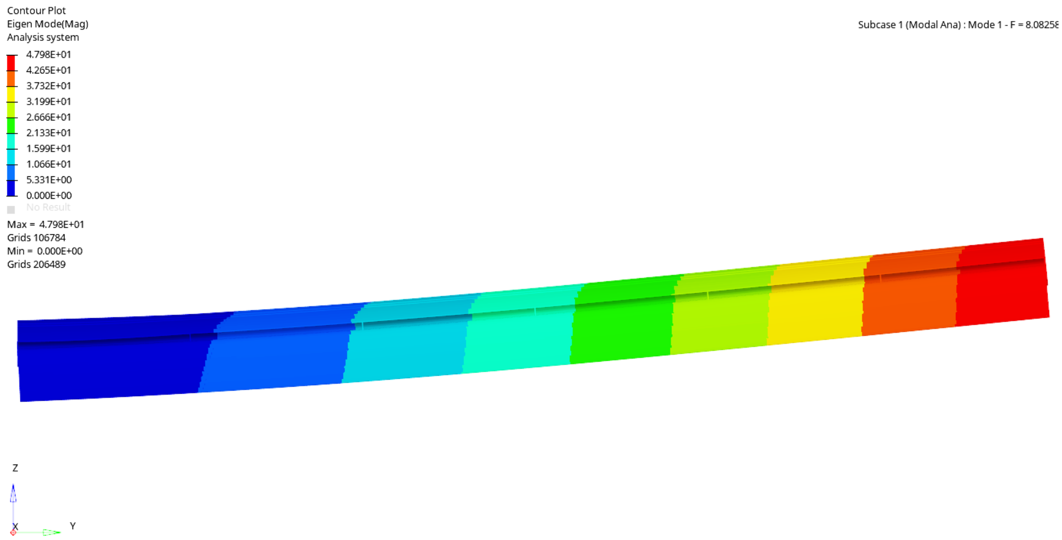
Contour Plot
Eigen Mode(Mag)
Analysis system
4.798E+01
4.265E+01
3.732E+01
3.199E+01
2.666E+01
2.133E+01
1.599E+01
1.066E+01
5.331E+00
0.000E+00
No Result
Max = 4.798E+01
Grids 106784
Min = 0.000E+00
Grids 206489
Subcase 1 (Modal Ana) : Mode 1 - F = 8.0825
Z
X
Y

(a)

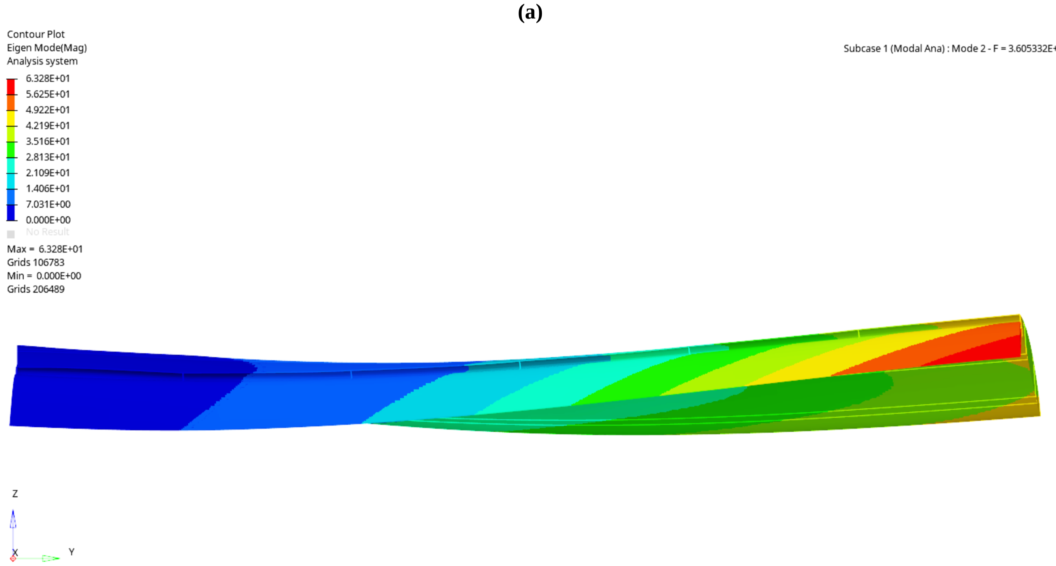
Contour Plot
Eigen Mode(Mag)
Analysis system
6.328E+01
5.625E+01
4.922E+01
4.219E+01
3.516E+01
2.813E+01
2.109E+01
1.406E+01
7.031E+00
0.000E+00
No Result
Max = 6.328E+01
Grids 106783
Min = 0.000E+00
Grids 206489
Subcase 1 (Modal Ana) : Mode 2 - F = 3.605332E+
Z
X
Y

(b)

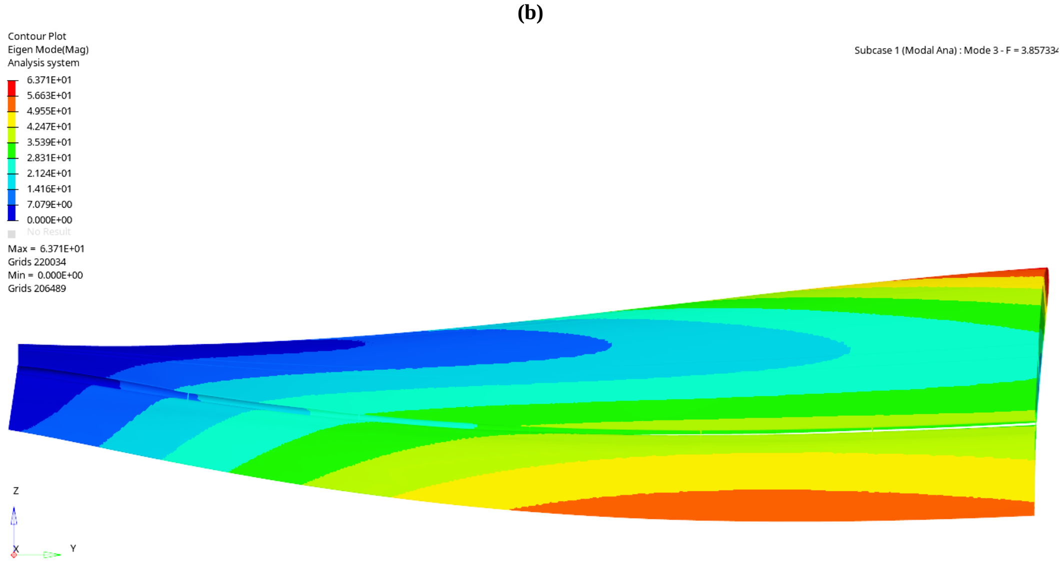
Contour Plot
Eigen Mode(Mag)
Analysis system
6.371E+01
5.663E+01
4.955E+01
4.247E+01
3.539E+01
2.831E+01
2.124E+01
1.416E+01
7.079E+00
0.000E+00
No Result
Max = 6.371E+01
Grids 220034
Min = 0.000E+00
Grids 206489
Subcase 1 (Modal Ana) : Mode 3 - F = 3.85733
Z
X
Y

(c)

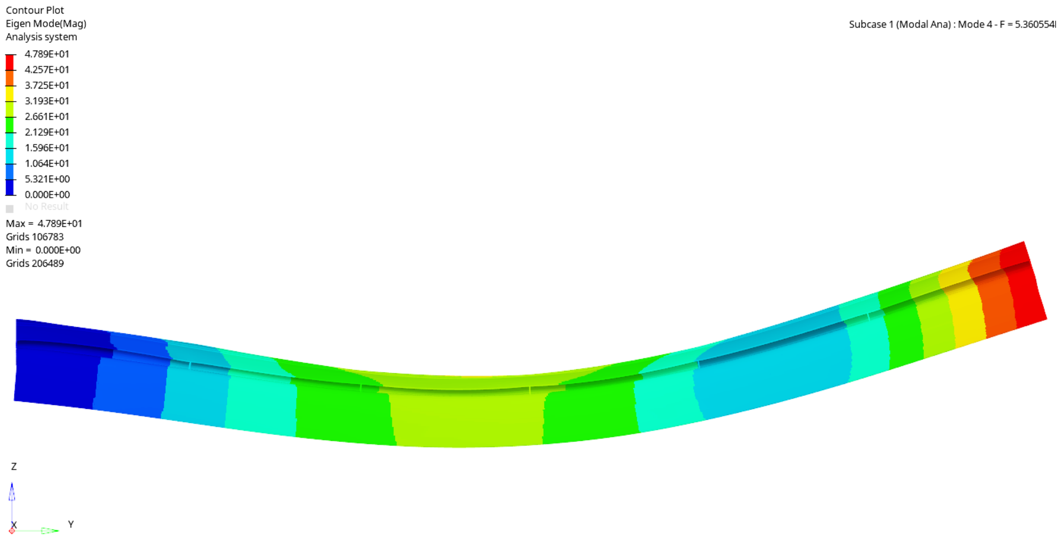

(d)

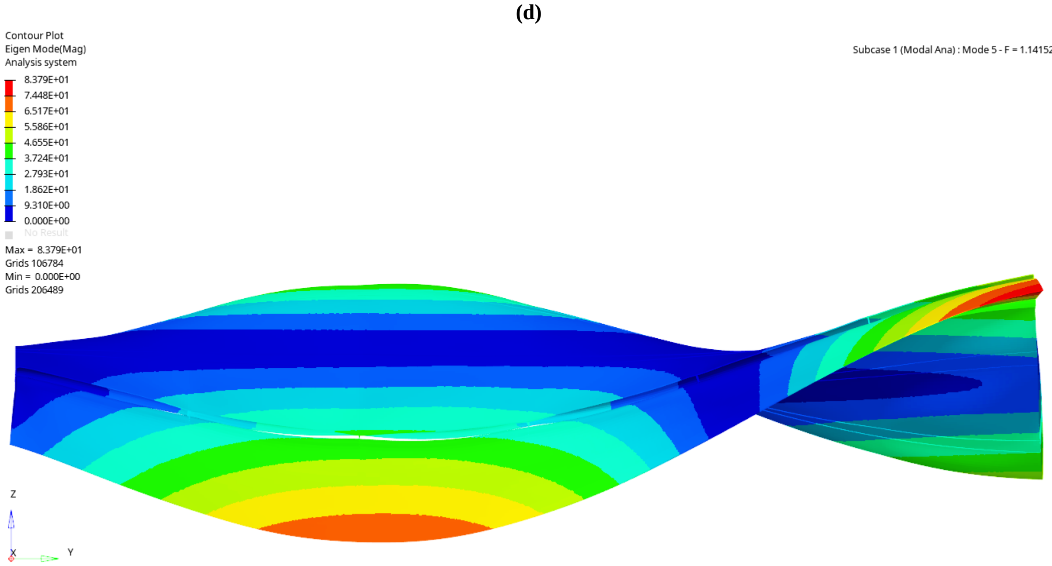

(e)

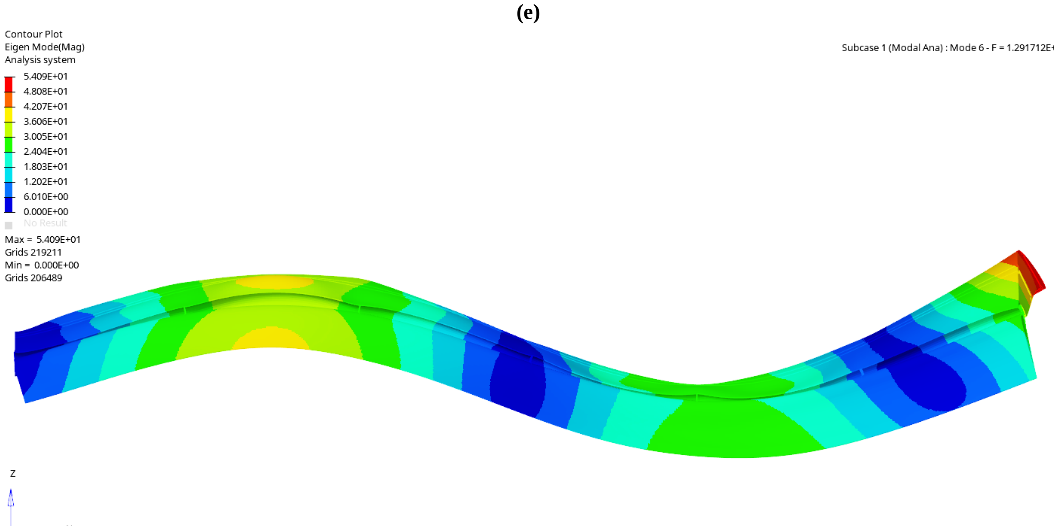

(f)

Fig. 8 Modal analysis of Carbon fiber (Hexcel AS4C) at the Flap

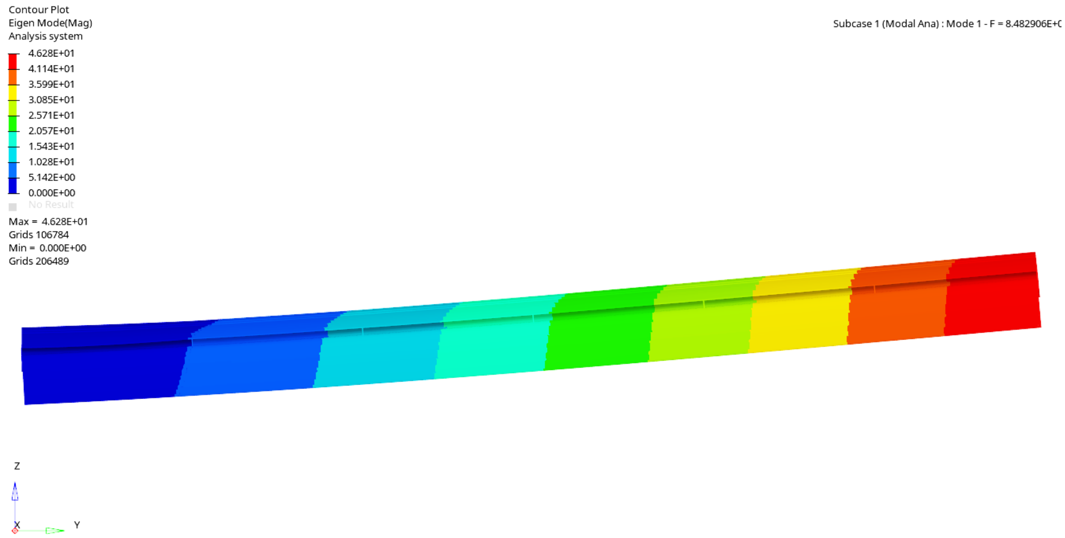
Contour Plot
Eigen Mode(Mag)
Analysis system
Subcase 1 (Modal Ana) : Mode 1 - F = 8.482906E+
4.628E+01
4.114E+01
3.599E+01
3.085E+01
2.571E+01
2.057E+01
1.543E+01
1.028E+01
5.142E+00
0.000E+00
No Result
Max = 4.628E+01
Grids 106784
Min = 0.000E+00
Grids 206489
Z
X
Y

(a)

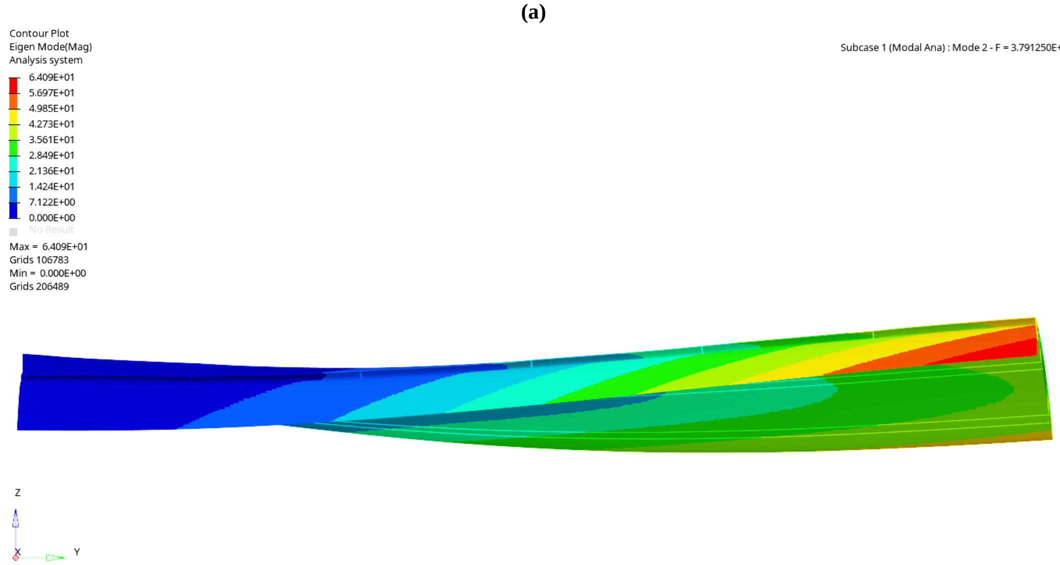
Contour Plot
Eigen Mode(Mag)
Analysis system
Subcase 1 (Modal Ana) : Mode 2 - F = 3.791250E+
6.409E+01
5.697E+01
4.985E+01
4.273E+01
3.561E+01
2.849E+01
2.136E+01
1.424E+01
7.122E+00
0.000E+00
No Result
Max = 6.409E+01
Grids 106783
Min = 0.000E+00
Grids 206489
Z
X
Y

(b)

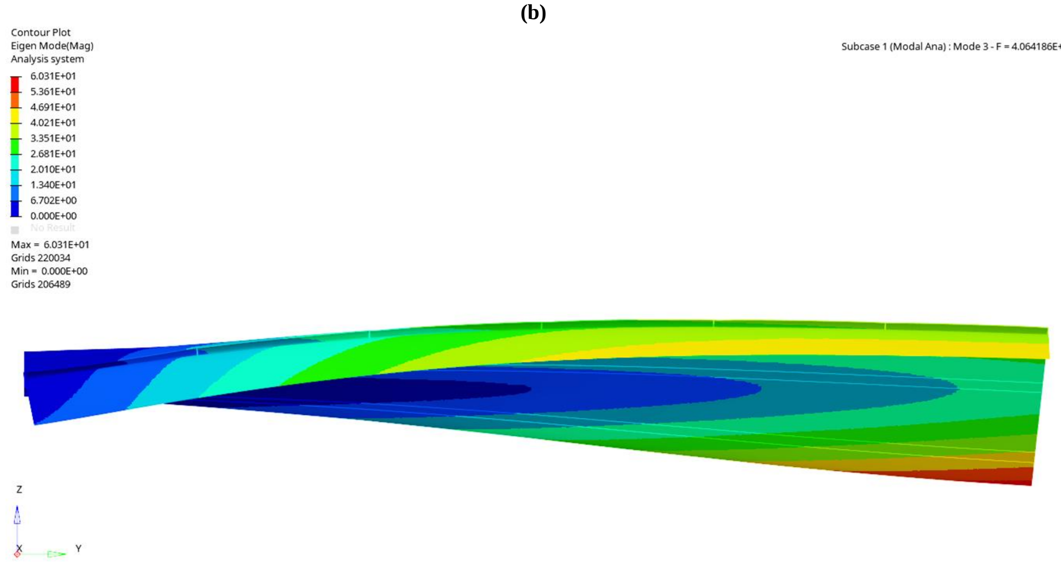
Contour Plot
Eigen Mode(Mag)
Analysis system
Subcase 1 (Modal Ana) : Mode 3 - F = 4.064186E+
6.031E+01
5.361E+01
4.691E+01
4.021E+01
3.351E+01
2.681E+01
2.010E+01
1.340E+01
6.702E+00
0.000E+00
No Result
Max = 6.031E+01
Grids 220034
Min = 0.000E+00
Grids 206489
Z
X
Y

(c)

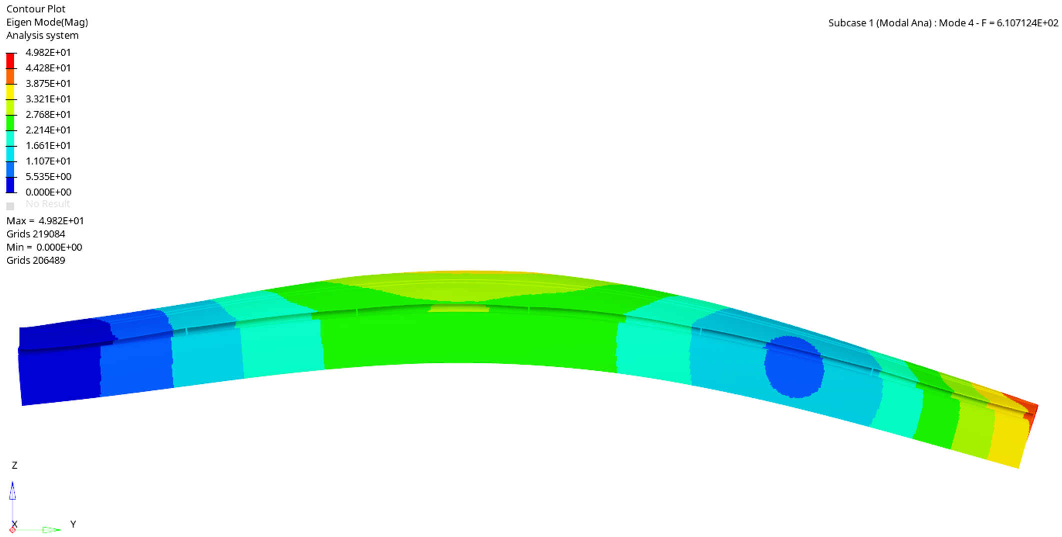

(d)

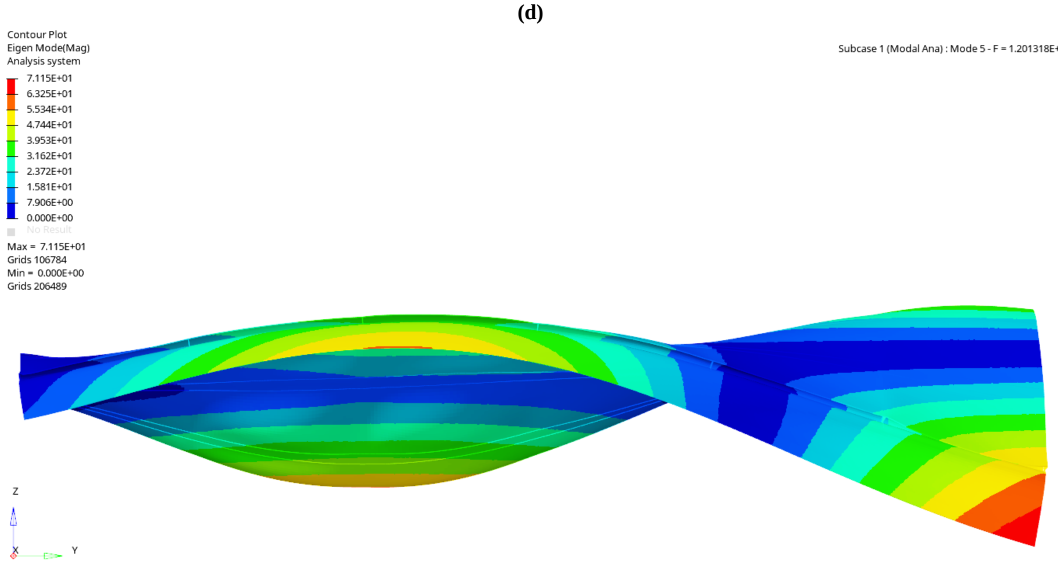

(e)

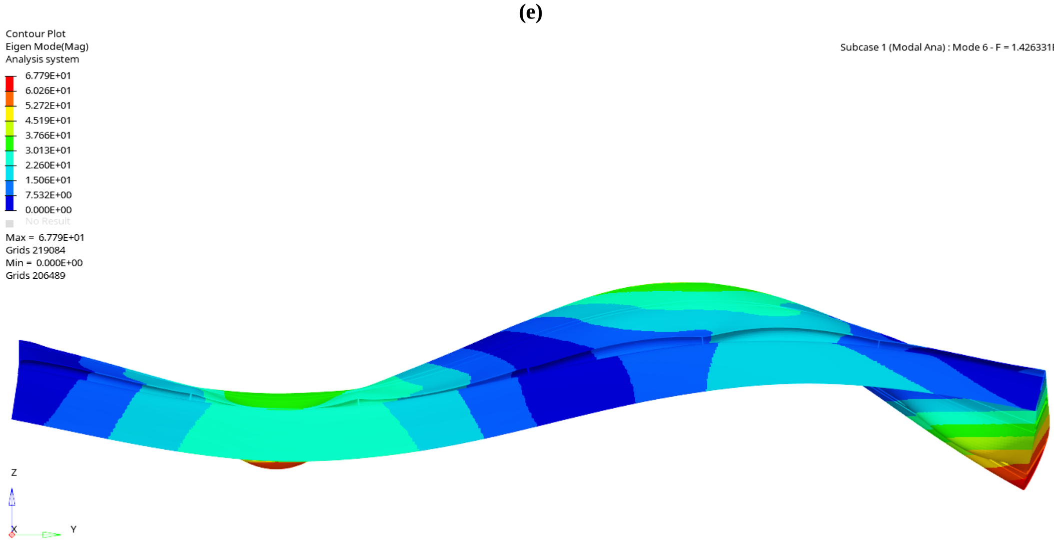

(f)

Fig. 9 Modal analysis of graphene at the Flap

The modal analysis gives valuable information about the dynamic behaviour of structures, such as Natural frequencies and mode shapes. Natural frequencies are the frequency where the structure vibrates when subjected to external forces. The natural frequency for each mode for three material types is listed in Table 4. The modal analysis also talks about the mode shapes, which show how the structure changes its shape and vibrates at various natural frequencies. Here, In Figures 7 to 9, the mode shape changes of the wing with flap section for different materials are shown for different natural frequencies. All the material has their maximum natural frequency in mode 6. Graphene has the maximum natural frequency than Al-2024 and Carbon fibre (Hexcel AS4C) in all 6 modes of frequencies. This shows that when graphene materials are used in a wing with a flap section, the entire structure does not vibrate more, and the rigidity of the structure increases comparatively. The pressure force acting on the wing and flap surface, which is given in Table 1, is taken from CFD analysis and given as the force acting on the surface of the wing and flap surface, and the results were taken. Three material properties are varied in the flap keeping the wing material as Al-2024.

Table 4. Natural frequency of materials

Modes & Frequency	Al-2024 All parts	Al- Wing, Spars & Ribs Carbon fiber (Hexcel AS4C) = Flap	Al- Wing, Spars & Ribs Graphene = Flap
Mode 1	72.616	80.825	84.829
Mode 2	320.137	360.533	379.125
Mode 3	341.514	385.733	406.418
Mode 4	452.298	536.055	610.712
Mode 5	889.708	1141.527	1201.318
Mode 6	1059.318	1291.712	1426.331

The static analysis for the wing with flap section where keeping the wing material constant to Al-2024 material and changing the flap section materials to Al-2024, carbon fiber and graphene are shown in Figures 10 to 12. The static analysis for a wing with a flap section which uses Al-2024 material is given in Figure 10. From the static analysis for the model, displacement, von Mises stress, maximum principal stress, von Mises strain, and maximum principal strain values are found. The displacement is more at the free end of the wing with a flap section, which is 6.98 for this case. Similarly, Von Mises stress and strain and Maximum Principal stress and strain values are found and it is given in Table 5. The static analysis for a wing with a flap section which uses carbon fiber (Hexcel AS4C) material is given in Figure 11. The displacement is more at the free end of the wing with the flap section as expected, which is 6.062 for this case. This value shows the rigidity of the structure.When the same force is applied to the structure with Al-2024 material, it deformed more compared to the carbon fiber (Hexcel AS4C) material configuration. The stress induced for the applied load in this configuration is less compared to the structure with the Al-2024 material configuration. The static analysis for a wing with a flap section, which uses Graphene material, is given in Figure 12. The displacement is more at the free end of the wing with flap section as expected, which is 5.247 for this case. From this value, we can understand that this configuration shows better structural rigidity Compared to the other two material cases. This configuration induces higher von Mises stress and strain and Principal stress values compared to the other two configurations. Commonly, the von Mises stress and strain and maximum principal stress and strain are more near the curved structure of the wing section, which is denoted with the red colour mark in Figures 10 to 12. Even though the stress-induced values are higher for the graphene materials, the structure does not fail which shows its capability of withstanding higher stress values without a failure.

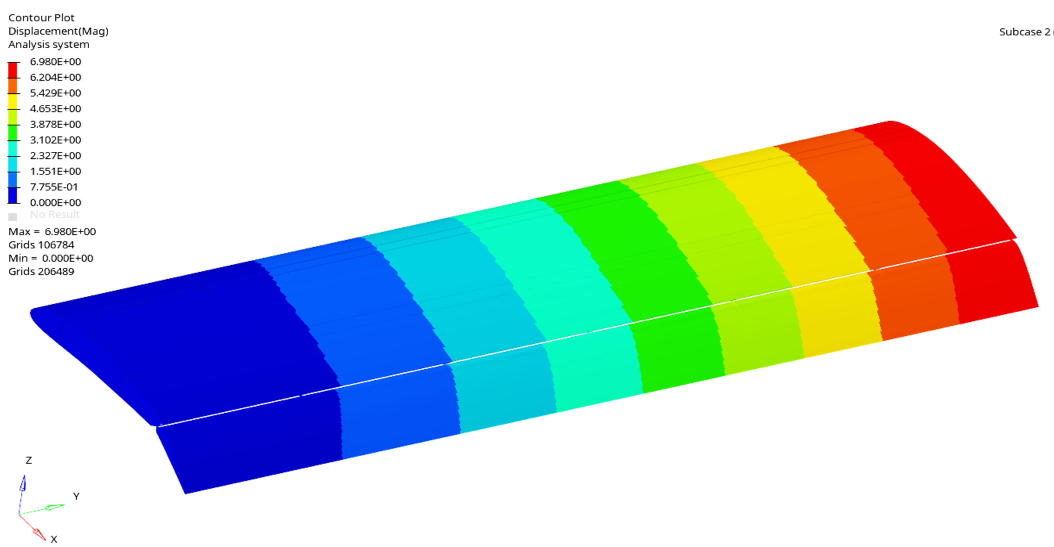

(a)

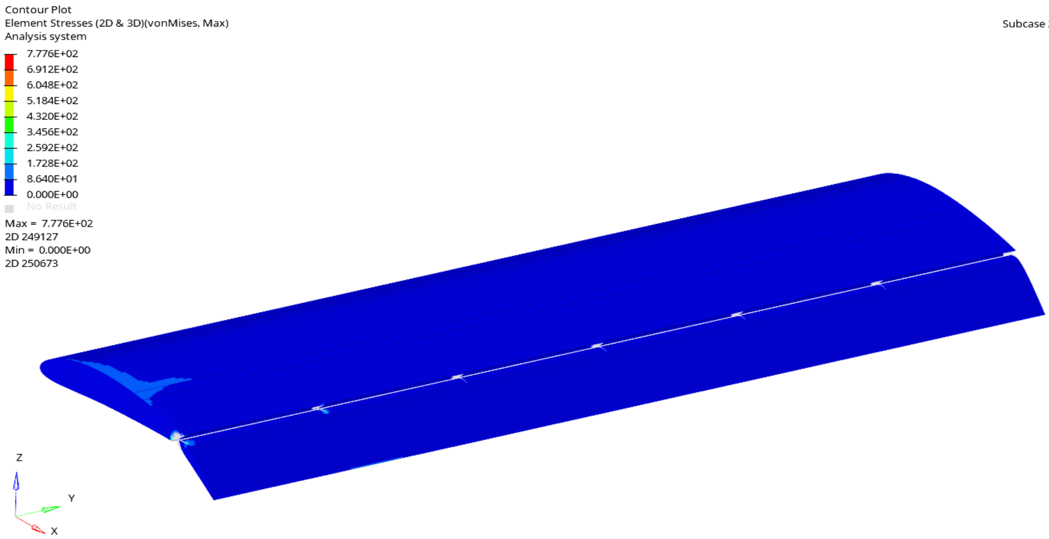
Contour Plot
Element Stresses (2D & 3D)(vonMises, Max)
Analysis system
Subcase 2
7.776E+02
6.912E+02
6.048E+02
5.184E+02
4.320E+02
3.456E+02
2.592E+02
1.728E+02
8.640E+01
0.000E+00
No Result
Max = 7.776E+02
2D 249127
Min = 0.000E+00
2D 250673
Z
Y
X

(b)

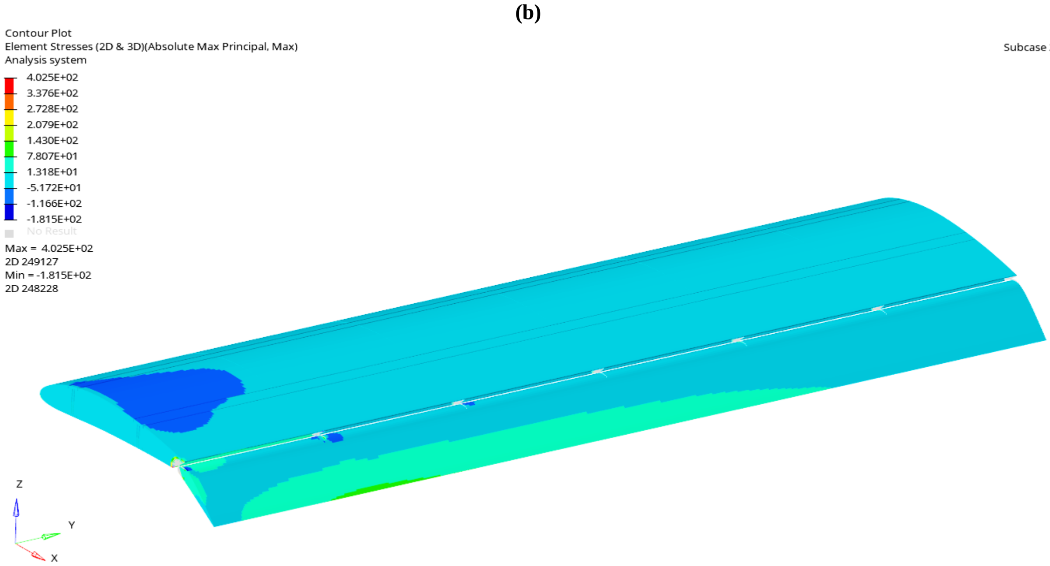
Contour Plot
Element Stresses (2D & 3D)(Absolute Max Principal, Max)
Analysis system
Subcase 2
4.025E+02
3.376E+02
2.728E+02
2.079E+02
1.430E+02
7.807E+01
1.318E+01
-5.172E+01
-1.166E+02
-1.815E+02
No Result
Max = 4.025E+02
2D 249127
Min = -1.815E+02
2D 248228
Z
Y
X

(c)

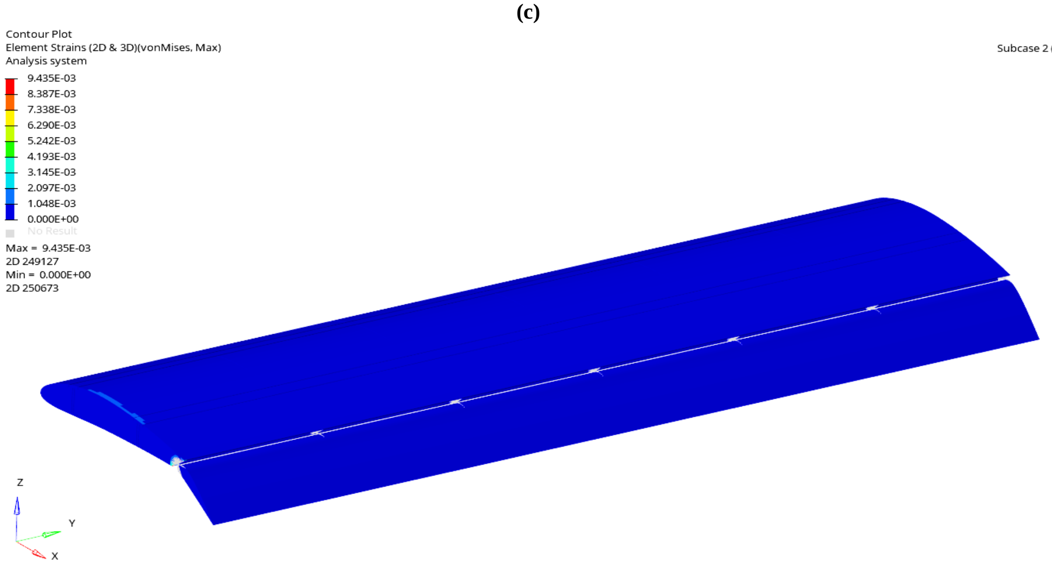
Contour Plot
Element Strains (2D & 3D)(vonMises, Max)
Analysis system
Subcase 2
9.435E-03
8.387E-03
7.338E-03
6.290E-03
5.242E-03
4.193E-03
3.145E-03
2.097E-03
1.048E-03
0.000E+00
No Result
Max = 9.435E-03
2D 249127
Min = 0.000E+00
2D 250673
Z
Y
X

(d)

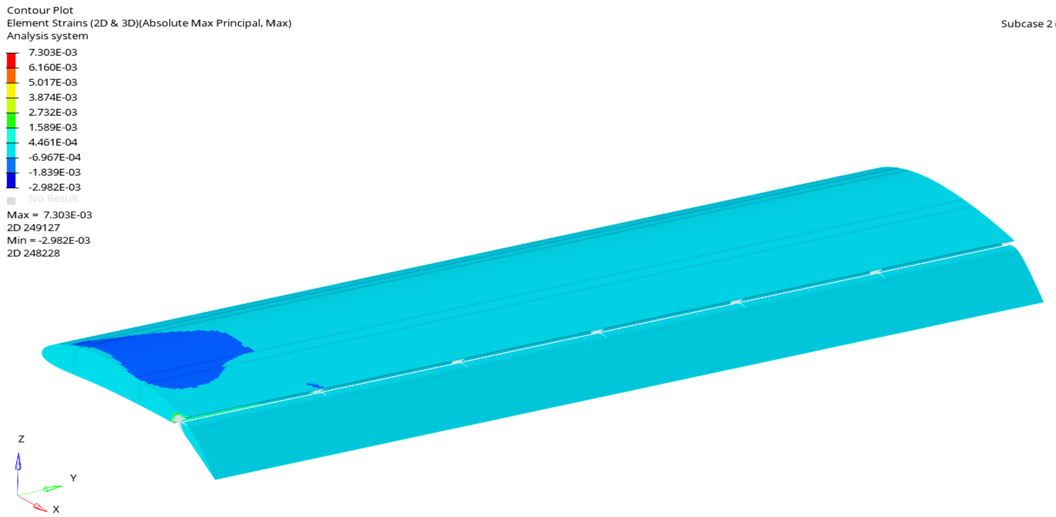

(e)

Fig. 10 Static analysis of Al-2024 material

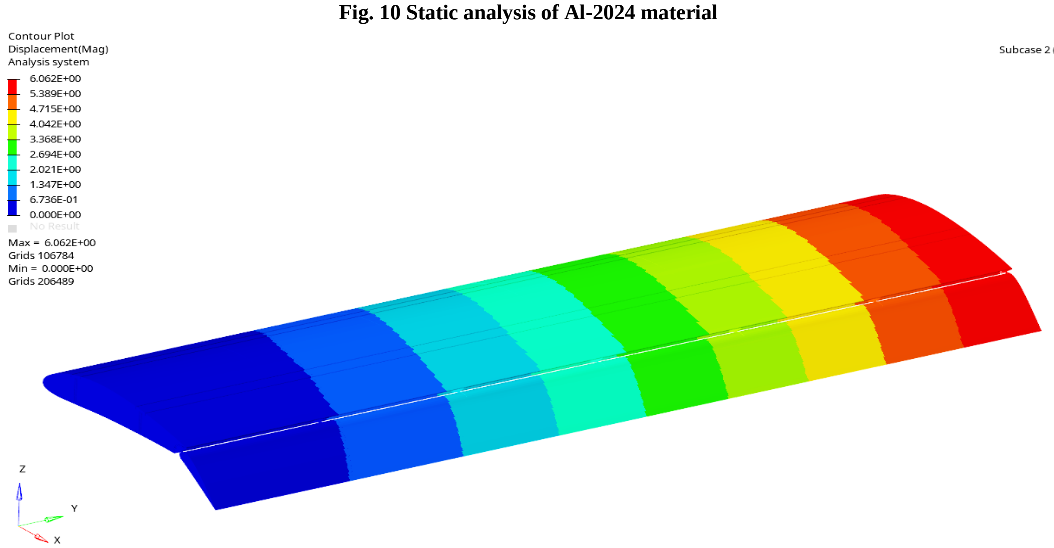

(a)

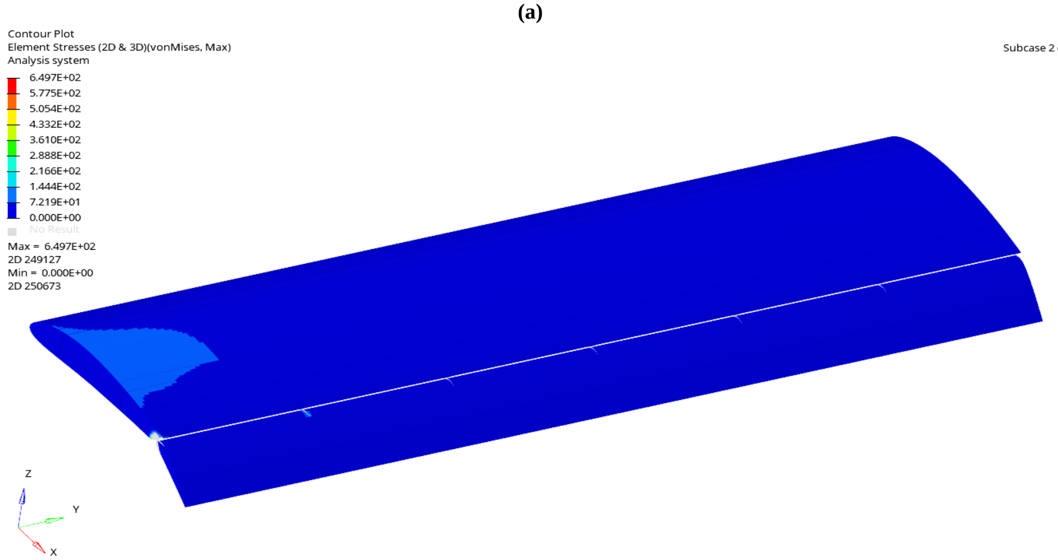

(b)

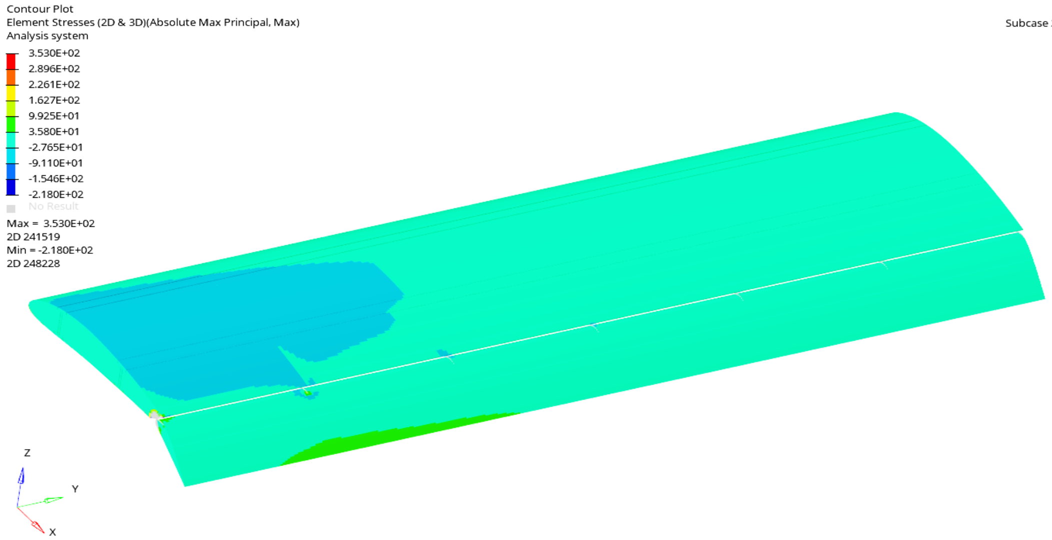

(c)

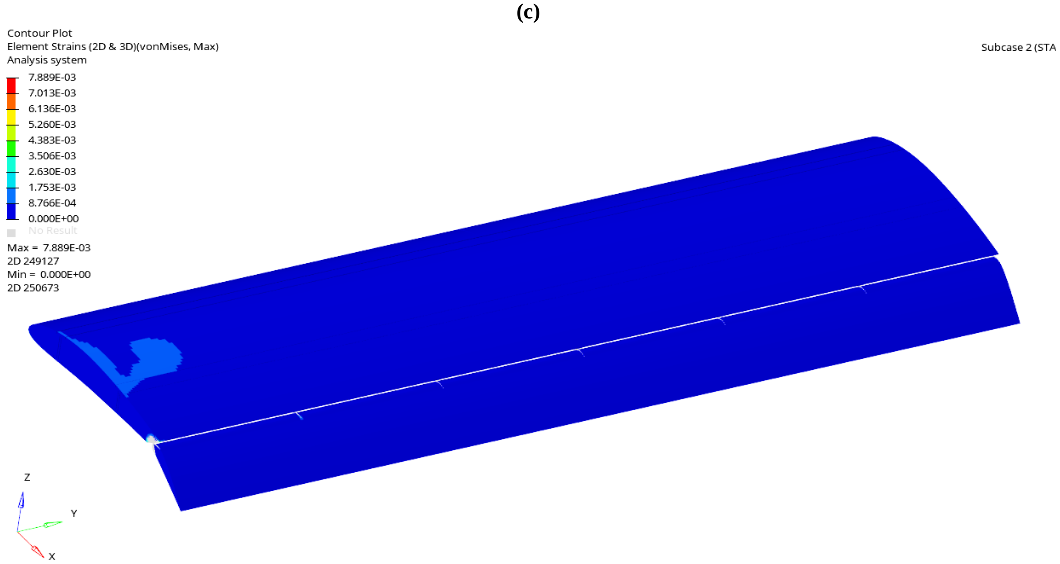

(d)

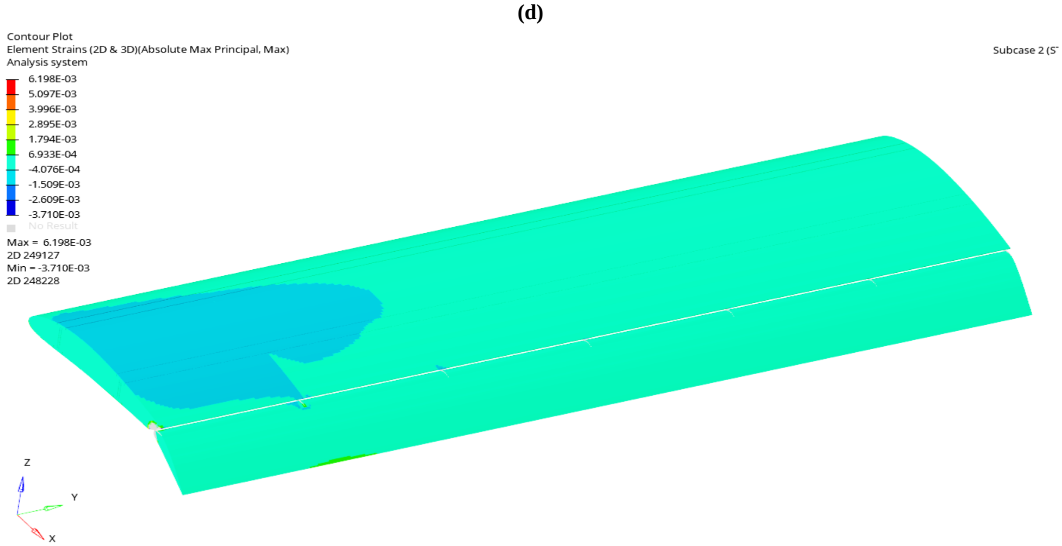

(e)

Fig. 11 Static analysis of Carbon fiber (Hexcel AS4C) at the Flap

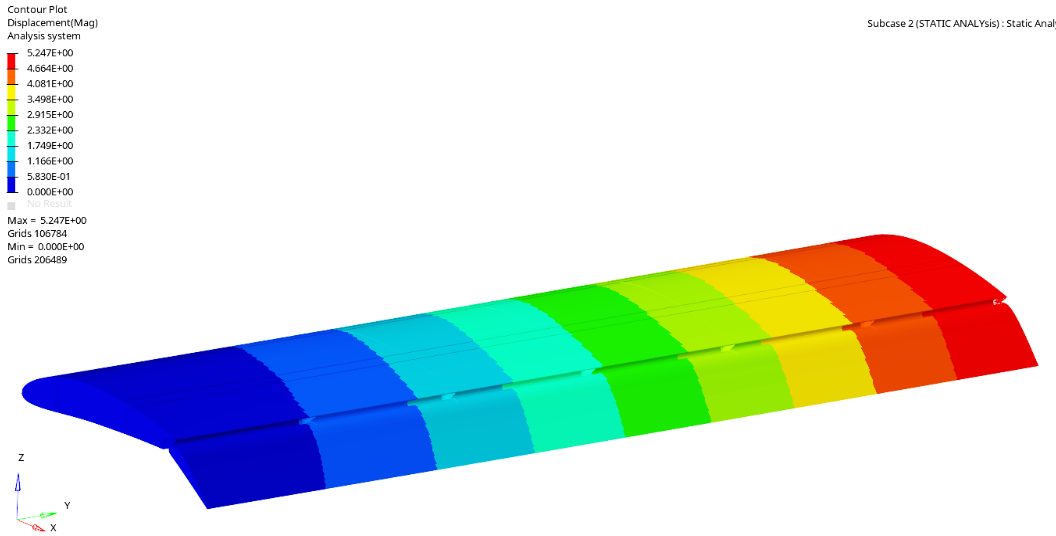
Contour Plot
Displacement(Mag)
Analysis system
Subcase 2 (STATIC ANALYsis) : Static Analy
5.247E+00
4.664E+00
4.081E+00
3.498E+00
2.915E+00
2.332E+00
1.749E+00
1.166E+00
5.830E-01
0.000E+00
No Result
Max = 5.247E+00
Grids 106784
Min = 0.000E+00
Grids 206489
Z
Y
X

(a)

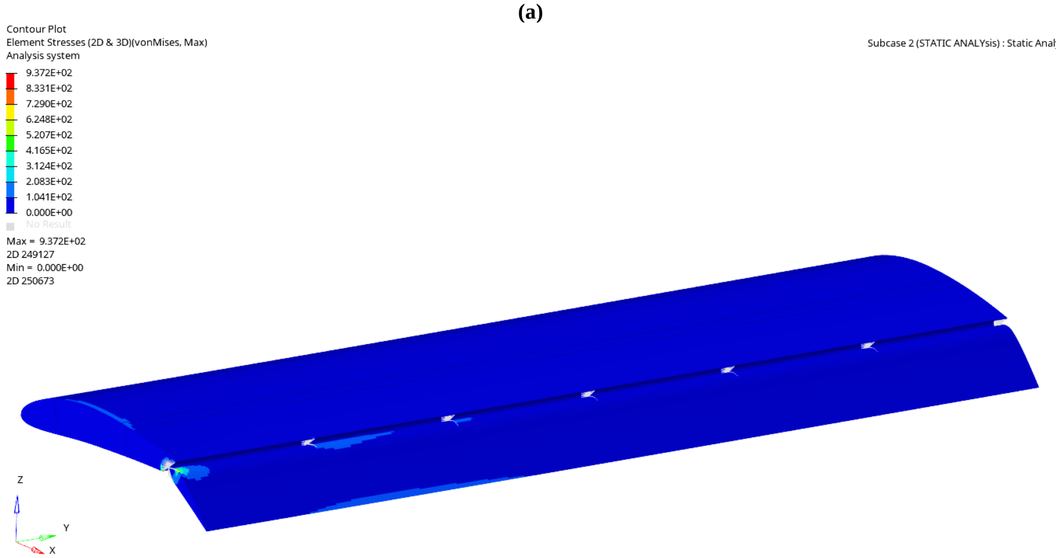
Contour Plot
Element Stresses (2D & 3D)(vonMises, Max)
Analysis system
Subcase 2 (STATIC ANALYsis) : Static Analy
9.372E+02
8.331E+02
7.290E+02
6.248E+02
5.207E+02
4.165E+02
3.124E+02
2.083E+02
1.041E+02
0.000E+00
No Result
Max = 9.372E+02
2D 249127
Min = 0.000E+00
2D 250673
Z
Y
X

(b)

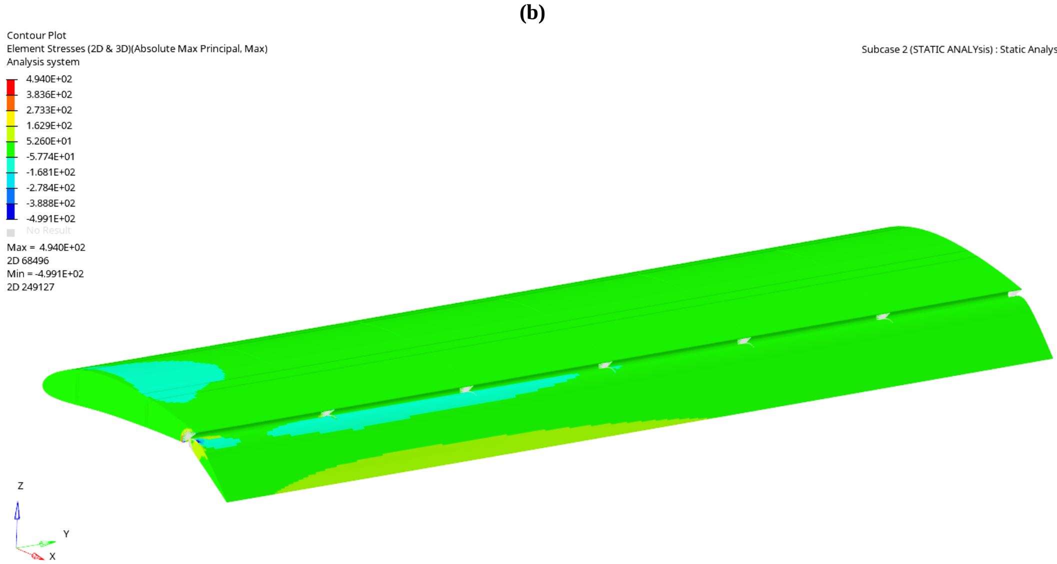
Contour Plot
Element Stresses (2D & 3D)(Absolute Max Principal, Max)
Analysis system
Subcase 2 (STATIC ANALYsis) : Static Analysi
4.940E+02
3.836E+02
2.733E+02
1.629E+02
5.260E+01
-5.774E+01
-1.681E+02
-2.784E+02
-3.888E+02
-4.991E+02
No Result
Max = 4.940E+02
2D 68496
Min = -4.991E+02
2D 249127
Z
Y
X

(c)

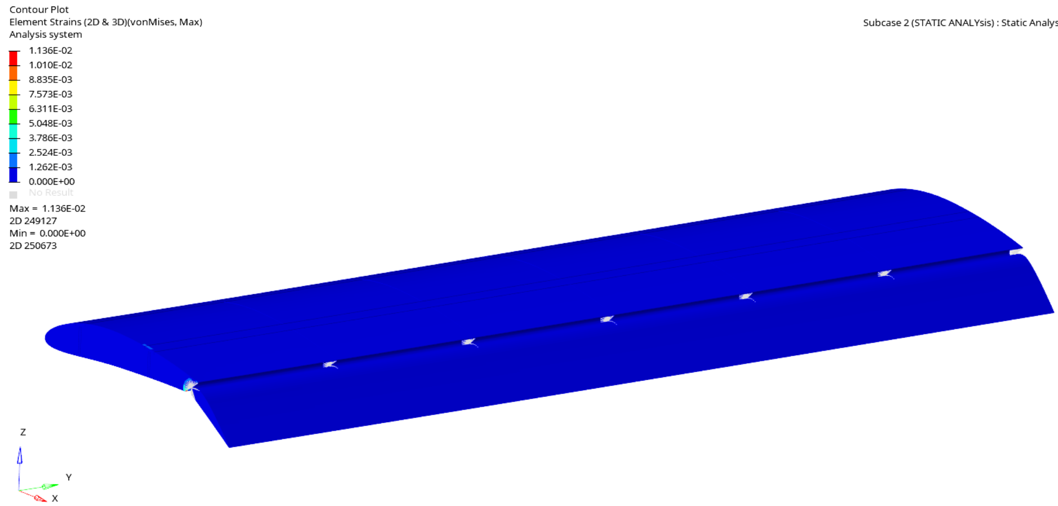

(d)

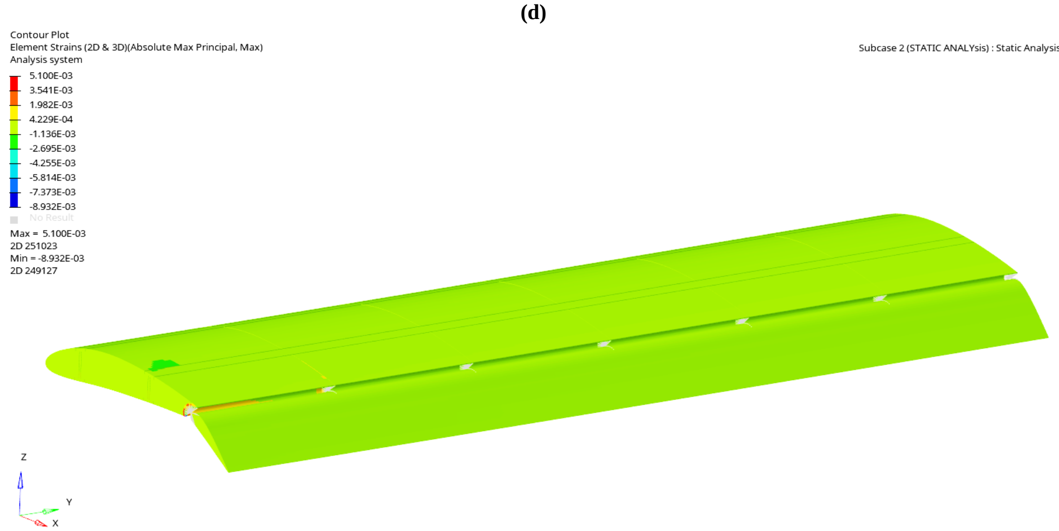

(e)

Fig. 12 Static analysis of graphene at the Flap

Table 5. Comparison of materials properties

Material Type	Displacement (mm)	Von-Mises Stress (N/mm2)	Maximum Principal Stress (N/mm2)	Von-Mises Strain (mm)	Maximum Principal Strain (mm)
Al-2024 All parts	6.98	7.77 E+02	4.025 E+02	0.009	0.007
Al- Wing, Spars & Ribs, Carbon fiber, (Hexcel AS4C)s = Flap	6.062	6.497 E+02	3.53 E+02	0.007	0.006
Al- Wing, Spars & Ribs, Graphene = Flap	5.247	9.37 E+02	4.94 E+02	0.011	0.005

6. Conclusion and Future work

In this research work, a wing with two spars and five ribs is modeled in CATIA, which is numerically analyzed, and the pressure values on the upper surface and the lower surface are taken for both the wing and flap. These pressure values are given as input in the structural analysis as a load. The modal and static analysis was done using HyperMesh Optistruct. Graphene has the maximum natural frequency of the other two materials. Graphene also has less strain and displacement compared to the other two materials when subjected to the same kind of loads; even though the stress value is more, the deformation is less; hence graphene can be used in the flaps instead of Al-2024 and Carbon fiber (Hexcel AS4C). Further, in future, Research can be carried out for any discontinuities in the wing or flap section and its fatigue strength can be compared. Different smart materials can be used, and results can be compared with graphene material results.

References

[1] Ajeet Kumar, Saurav Verma, and Jeng-Yawn Jeng, "Supportless Lattice Structures for Energy Absorption Fabricated by Fused Deposition Modeling," *3D Printing and Additive Manufacturing*, vol. 7, no. 2, pp. 85-96, 2020. [CrossRef] [Google Scholar] [Publisher Link]

[2] Arnav Kulshreshtha, Sanjeev Kumar Gupta, and Piyush Singhal, "FEM/CFD Analysis of Wings at Different Angle of Attack," *Materials Today: Proceedings*, vol. 26, pp. 1638-1643, 2020. [CrossRef] [Google Scholar] [Publisher Link]

[3] Bartlomiej Przybyszewski et al., "A Wind Tunnel Experimental Study of Icing on NACA0012 Aircraft Airfoil with Silicon Compounds Modified Polyurethane Coatings," *Materials*, vol. 14, no. 19, pp. 1-15, 2021. [CrossRef] [Google Scholar] [Publisher Link]

[4] Caner Senturk, Mehmet Șerif Kavsaoglu, and Melike Nikbay, "Optimization of Aircraft Utilization by Reducing Scheduled Maintenance Downtime," *10th AIAA Aviation Technology, Integration, and Operations (ATIO) Conference*, Fort Worth, Texas, 2010. [CrossRef] [Google Scholar] [Publisher Link]

[5] Nitin Chandola, and Rohit Singh Rawat, "Finite Element Analysis of Wing Design," *Proceeding of International Conference on Intelligent Communication, Control and Devices*, pp. 503-509, 2016. [CrossRef] [Google Scholar] [Publisher Link]

[6] Christopher L. Rumsey, and Susan X. Ying, "Prediction of High Lift: Review of Present CFD Capability," *Progress in Aerospace Sciences*, vol. 38, no. 2, pp. 145-180, 2002. [CrossRef] [Google Scholar] [Publisher Link]

[7] David Zaccai, Francesco Bertels, and Roelof Vos, "Design Methodology for Trailing-Edge High-Lift Mechanisms," *CEAS Aeronautical Journal*, vol. 7, pp. 521-534, 2016. [CrossRef] [Google Scholar] [Publisher Link]

[8] R. Rajappan, and V. Pugazhenthi, "Finite Element Analysis of Aircraft Wing Using Composite Structure," *The International Journal of Engineering and Science*, vol. 2, no. 2, pp. 74-80, 2013. [Google Scholar] [Publisher Link]

[9] R. Rajendran et al., "Analysis of Morphing Airfoil Structures and Fabrication of the Wing using the Concept of Additive Manufacturing," *International Journal of Engineering Research & Technology*, vol. 9, no. 6, pp. 54-58, 2020. [Publisher Link]

[10] Girish Chandrakant Mekalke, and A.V. Sutar, "Modal Analysis of Cantilever Beam for Various Cases and its Analytical and FEA Analysis," *International Journal of Engineering Technology, Management and Applied Sciences*, vol. 4, no. 2, pp. 60-66, 2016. [Google Scholar]

[11] Guanghao Li et al., "Graphene Based Self-Healing Materials," *Carbon*, 146, Vol. 146, pp. 371-387, 2019. [CrossRef] [Google Scholar] [Publisher Link]

[12] John O. Akindoyo et al., "Polyurethane Types, Synthesis and Applications – A Review," *Royal Society of Chemistry*, vol. 6, no. 115, pp. 114453-114482, 2016. [CrossRef] [Google Scholar] [Publisher Link]

[13] Kenneth Witcher, Ian McAndrew, and Elena Visnevskaya, "Aerodynamic Analysis of Low Speed Wing Design using Taguchi L9 Orthogonal Array," *MATEC Web of Conference*, vol. 151, 2017. [CrossRef] [Google Scholar] [Publisher Link]

[14] V. Pugazhenthi, S. Gopalakannan, and R. Rajappan, "Finite Element Analysis of Composite Shell Structure of Aircraft Wing Using Composite Structure," *2018 IEEE International Conference on System, Computation, Automation and Networking*, Pondicherry, India, pp. 1-8, 2018. [CrossRef] [Google Scholar] [Publisher Link]

[15] Yupeng Li et al., "A Review on Room-Temperature Self-Healing Polyurethane: Synthesis, Self-Healing Mechanism and Application," *Journal of Leather Science and Engineering*, vol. 4, no. 1, 2022. [CrossRef] [Google Scholar] [Publisher Link]

[16] Salu Kumar Das, and Sandipan Roy, "Finite Element Analysis of Aircraft Wing using Carbon Fiber Reinforced Polymer and Glass Fiber Reinforced Polymer," *2nd International Conference on Advances in Mechanical Engineering*, *IOP Conference*, vol. 402, no. 1, 2018. [CrossRef] [Google Scholar] [Publisher Link]

[17] G. Saravanan, A. Arul Johnson, and P. Pandiarajan, "Finite Element Analysis of Aircraft Wing Joint and Fatigue Life Prediction Under Variable Loading using MSC Patran And Nastran," *International Journal of Mechanical Engineering and Technology*, vol. 9, no. 11, pp. 1111-1119, 2018. [Google Scholar] [Publisher Link]

[18] Sivarama Prasad Peruru, and Suman Babu Abbisetti, "Design and Finite Element Analysis of Aircraft Wing Using Ribs and Spars," *International Research Journal of Engineering and Technology*, vol. 4, no. 6, pp. 2133-2139, 2017. [Google Scholar] [Publisher Link]

[19] Sravan Kumar Khuntia, and Amandeep Singh Ahuja, "Optimal Design and CFD Analysis of Wing of a Small-Scale UAV to Obtain Maximum Efficiency," *Journal of Aeronautics & Aerospace Engineering*, vol. 7, no. 1, pp. 1-7, 2018. [CrossRef] [Google Scholar] [Publisher Link]

[20] Tseko Mofokenga, Paul T. Mativenga, and Annlize Marnewick, "Analysis of Aircraft Maintenance Processes and Cost," *27th CIRP Life Cycle Engineering (LCE) Conference*, *Procedia CIRP*, vol. 90, pp. 467-472, 2020. [CrossRef] [Google Scholar] [Publisher Link]

[21] P. Vinay Kumar et al., "Design and Finite Element Analysis of Aircraft Wing Using Ribs and Spars," *Turkish Journal of Computer and Mathematics Education*, vol. 12, no. 8, pp. 3224-3230, 2021. [Google Scholar] [Publisher Link]